Technical Energy Potential Of Floating PV Power Plants (FPV)

Ahmed Mostafa

Matriculation Nr.: 42366

Under the supervision of:

Dr.-ing. Sebastian Voswinckel

Ing. Lukas Gerstenberg

A thesis presented for the degree of
Masters of Engineering (M. Eng.)

Renewable Energy System RES
Hochschule Nordhausen
The University of Applied Sciences

May 11, 2021

Table of contents

Symbol	Unit	Meaning
T_m	$^\circ C$	PV Module temperature
T_a	$^\circ C$	Ambient temperature
T_s	$^\circ C$	Temperature of surface
T_f	$^\circ C$	Temperature of fluid
T_r	$^\circ C$	Temperature of radiator
T_c	$^\circ C$	Temperature of receiver
T_e	$^\circ C$	Effective temperature
T_{sky}	$^\circ C$	Sky temperature
T_m	$^\circ C$	PV module temperature
T_g	$^\circ C$	Ground-surface temperature
T_w	$^\circ C$	Water-surface temperature
RTI	W/m^2	Reflected Tilted Radiation
GHI	W/m^2	Global Horizontal radiation
ρ_A	%	Albedo value
γ_m	$^\circ$	tilt angle of the module
V_{oc}	$volt$	Open circuit voltage
$V_{oc,STC}$	$volt$	Open circuit voltage at the standard test conditions
β	$\%/\ ^\circ C$	Temperature coefficient of PV module for the voltage
T_{STC}	$^\circ C$	Standard test condition temperature
I_{sc}	$Ampere$	Short circuit current
$I_{sc,STC}$	$Ampere$	Short circuit current at the standard test conditions
α	$\%/\ ^\circ C$	Temperature coefficient of PV module for the current
k	W/mK	Thermal conductivity
h_c	W/m^2K	Convection heat transfer coefficient
h_r	W/m^2K	Radiative heat transfer coefficient
h	W/m^2K	Overall heat transfer coefficient
σ	W/m^2K^4	Stefan's constant
G	W/m^2C	Global radiation
G_r	W/m^2C	Reflected solar radiation
ΔR	W/m^2C	Thermal radiation
V	m^2/s	Wind speed
N	1	Cloudiness of the sky
α_0	1	Abosrbitivity
ε	1	Emissivity
$\eta_{c_{FPV}}$	%	FPV cell efficiency
$\eta_{c_{GPV}}$	%	GPV cell efficiency
η_{Tref}	%	Reference cell efficiency
$\dot{q}$	W/m^2	Net heat transfer
$\dot{q_c}$	W/m^2	Convective heat transfer
$\dot{q_r}$	W/m^2	Radiativee heat transfer
P_{FPV}	W_p	FPV cell efficiency
P_{GPV}	W_p	GPV cell efficiency

List of abbreviations

in.RET Institut for Regenerative Energietechnik

FPV Floating Photovoltaic

GPV Ground-mounted Photovoltaic

FIT Feed-In-Tariff

FTCC Floating Tracking Cooling Concentrating

EVA Ethylene-Vinyl-Acetate

List of Figures

List of Tables

Abstract

Energy demand is significantly expanding worldwide nowadays, as a result the capacity of the electricity generating units come into question. Based on the World Energy Balances Highlights (2020 edition) [19], it was found that the world electricity generation is about $26,618,881\ GWh$ from all sources proposed i.e. "Fossil fuels, Nuclear, Renewable Energies". Consequently,there would be too much negative effects on the environment due to the continuous usage of fossil contents which are used later for the electricity generation. The electric sector obsessed about 42 % of the energy demand in 2015 and it is expected to raise to 47 % in the next 20 years. It is remarkable that the non-renewable sources of energy affect the environment negatively and increase the global warming when they are used for the generation of the electricity.

Despite the constantly increasing of the electricity demand, the dependency of the non-renewable sources on energy must be reduced in order to lower the amount of the greenhouse gases. In 2018, the renewable energy generation share has became 13.5 % of the total world energy supply including (Solar PV, Solar thermal, Wind, Bio-fuels, Hydro, and Geothermal energies) [19]. The solar photovoltaic power generation has increased by about 22 % in 2019, and namely to 720 TWh. It can be considered by this increase as 3 % of the total world electricity generation share. In the meanwhile, the main challenge of installing normal ground-mounted PV power plants is the space. Large surface areas must be available in order to benefit well from such power plants. In order to tackle this issue, another generation of PV power plants came into question which is; Floating Photovoltaic (FPV).

This technology depends on installing the PV modules over the surface of water, in order to profit not only from the extra space where water body is located, but also from the cooling effect, which improves the performance of PV modules and particularly, the performance ratio as well as the electrical efficiency. Furthermore, a tracking model can be easily applied to this kind of PV, since the surface of water offers a smooth medium for changing the modules orientation over the whole day.

The floating photovoltaics have a lot of benefits over the ground-mounted type, for example; the land occupancy, as they do not require a land space, since they are installed and erected on the surface of water, except only the needed spaces which are demanded by the electrical equipment, switch gears. Although, FPV plants are considered relatively more expensive than the land-based photovoltaic power plants, but they empower the possibility to avoid competing with the agriculture and green zones. Moreover, to prevent the competing with the agriculture and green lands, some countries encourage the investors to install PV on the water bodies by increasing the rate of incentives. For instance, Japan has boosted the Feed-In-Tariff (FIT) for the floating photovoltaic over the FIT of the ground-mounted PV. In particular, the floating PV array in Sanuki, Kagawa prefecture, which has an installed capacity of 1.5 MW and expected to meet the consumption of more than 500 local households, will purchase the electricity at a Feed-In-Tariff of JPY 32 per kWh ($0.26\ €/kWh$)[20].

In this work, two main models are built in order to calculate the PV module temperature and the surface temperature of the ground and water in order to; 1) determine the how the surface temperature of the ground and water affects the module temperature and namely the output power, 2) predict the temperature of both FPV, 3) calculate the to the instantaneous efficiency and power of the FPV and GPV modules, and 4) predict the annual yield of floating PV module

Chapter 1

Key benefits of the floating photovoltaic

Floating solar photovoltaic panels work with the same concept as the ground-mounted panels, except that they are mounted on the surface of the water, either on man-made surfaces or on the surface of natural water bodies. However, the floating photovoltaic must fit onto the floaters, which offer the support, orientation, and the required tilt angle for the panels for example in case of pontoon structure, as for other types of FPV the tilt angle and the support of PV modules is made by means of an extra under-construction over the floaters.

Figure 1.1: Floating Power Plant (FPV)

Solar panels on the water surface work better than the ground-mounted because of the low operating temperature of the cells. However, floating photovoltaic (FPV) offers a lot of benefits with particular regarding environment, water condition, and the amount of the harvested energy. Those advantages are detailed as the following:

1.1 Land use and occupancy

The unique advantage of the floating or submersed photovoltaic power plants is that, they do not require a land space, as they are installed and erected on the surface of water, except only the needed spaces which are demanded by the electrical equipment, switch gears. Although, FPV plants are considered relatively more expensive than the land-based photovoltaic power plants, but they empower the possibility to avoid competing with the agriculture and green zones.

Furthermore, for countries where land is not suitable for setting up a ground-mounted PV, the costs increase significantly, as the land is required first to be settled to be appropriate enough for the installation (For countries where terrains are unsuitable for the deployment of PV). Additionally, for small countries where the energy demand is high and the access of grid electricity is relatively hard, the installation of a ground-mounted PV becomes sometimes difficult as the plant becomes far away from the nearest grid connection. In such cases, a connection to the high voltage grid is required, which is at the end not only inefficient and very expensive, but also a certain percentage of energy is lost during the transmission. On the other hand, trying to install PV ground-mounted plants nearby or close to inhabited areas is also expensive. For example, in China, the government restricts the installation of ground-mounted PV as they threaten agriculture and green areas. Therefore, FPV is considered as a unique and feasible solution. It deploys the water bodies, which are not economically required, in addition that, they can be leased with no or very low cost.

Moreover, to prevent the competing with the agriculture and green lands, some countries encourage the investors to install PV on the water bodies by increasing the rate of incentives. For instance, Japan has boosted the Feed-In-Tariff (FIT) for the floating photovoltaic over the FIT of the ground-mounted PV. In particular, the floating PV array in Sanuki, Kagawa prefecture, which has an installed capacity of 1.5 MW and expected to meet the consumption of more than 500 local households, will purchase the electricity at a Feed-In-Tariff of JPY 32 per kWh ($0.26 \text{€}/kWh$)[20].

1.2 Erection and commissioning

The floating photovoltaic plants (FPV) are considered more integrated and compact than the ground-mounted ones. For example, the floating PV power plants which use Pontoon-mounted solar modules Figure 1.2, as the modules not only can be easily mounted and integrated into pontoons, but also the decommissioning process is not complicated. Furthermore, the erection and mooring processes are considered completely reversible, which means that they can be easily decommissioned. Each floater row must be integrated with the solar module and only before being thrown into water, and only after integrating the whole plant modules into the pontoons, the array must be led to its assigned location using steel ropes and a ship.

However, this process is considered as not so hectic because water enables enough flexibility to transport and lead the while array to the required location. Subsequently, the technicians can move through the plant in order that they complete the electrical connections and wiring or for the purpose of testing and maintenance. However, there must be a pathway allows the possibility of reaching the floating power plant starting from the land if the FPV is not far away from the land, otherwise, ships are used.

Figure 1.2: Pontoon type floating photovoltaic [1]

In the meanwhile, it is projected that about 70 % of the amount of water on earth is used directly for the irrigation purposes, with 15-35 % of that percentage is considered non-renewable. Around 2,000 and 3,000 liters per day are required for cooking and from 2 to 5 liters per day for drinking purpose. On the large industrial scale, about 22 % is necessary for the industrial customers. Namely, hydroelectric power plants, thermal power plants, steam plants which use water either as a main fluid for generating electricity or for cooling the moving equipment, and another industrial sectors, like oil refineries which use water in chemical processes, and the rest percentage is for households usages.

There is no doubt among these pathways that water bodies are suffering from the extreme evaporation. Some of the methods which are used for reducing the water evaporation is the coverage of water surface. The quality of water is highly influenced by the partial or full coverage of surface. As a result, a big amount of water can be saved, especially if the water body is used for irrigation purposes. As shown in Figure 1.3, the evaporation rate of water is highly affected by the ambient temperature and the solar irradiation, that means, the evaporation rate of water increases with the increasing of the temperature.

Furthermore, about 80 % of water evaporation was saved in Australia (More than $20,000$ m^3/year/hectare [21]. Not only that, but also the covering of water surface using FPV provides enough shading that helps in limiting the growing of algae, since they are not desirable as they impede the pumping and filtering systems.

1.3 Water cooling effect

The PV modules as well as the energy efficiency are highly influenced by the temperature. Installing the PV on the water bodies increases the efficiency since the temperature is lower than the normal ground temperature. The more water evaporates and turns from the liquid into the steam phase the more water cooling effect is generated, as the water molecules require heat in order to escape and convert into steam. It was investigated by literature that the solar modules lose their efficiency during the hot seasons because of the thermal drift effect [21].

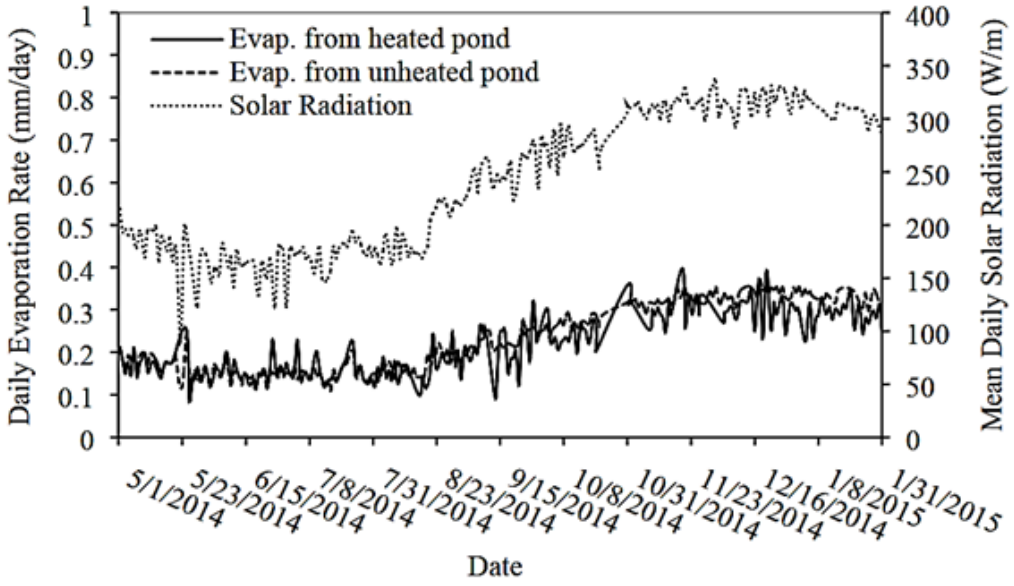

Figure 1.3: Water evaporation rate for a heated and unheated ponds [2]

However, the thermal drift lowers the efficiency of module by $10 - 15$ % during the hot seasons (For example: The Summer season), despite the high irradiation [5].

Table 1.1 shows a summary of the differences of efficiency of FPV than the ground-mounted PV (GPV) (See chapter 3).

For example in [15] the author has performed the following three case studies;

- Ground-mounted PV plant which is located near to a lake oriented directly to the south, and with a fixed tilt angle of 30°.
- Base-Concept FPV installed over the surface of the lake with a fixed optimum azimuth angle of 0° and an optimum tilt angle of 12°
- Proposed-Concept FPV also on the lake surface with a variable azimuth angle and an optimum tilt angle of 44°

As a result, they performed a comparison between the three case study models with the final harvested energy GWh as well as the annual insolation kWh/m^2/day for each scenario as shown in table 1.2.

The overall energy yield difference between the first scenario (Ground-mounted PV) and the (Proposed floating PV (FPV)) is 44.34 GWh which represents 31.289 % extra for the floating PV.

[23] has made a a case study on the first project which is exposed to the ice and snow. The project is grid-connected in Italy with 500 kW_p and was erected in 2009 by the collaboration of local companies. The developer companies claim 20-25 % gain of the generated electricity out of the plant.

In [3], a multi-linear optimization was performed to predict the optimum energy out of the FPV

Table 1.1: Reviews on the efficiency differences between FPV over GPV

Autor	**Reference**	**Efficiency difference (%)**
Choi, Lee, et al. 2013	[22]	10.3,13.5, and 11
Durkovi´c, Djurisic et al. 2015	[15]	31.29
Trapani, Santafé et al. 2015	[23]	20.0–25.0
Spencer, Macknick et al. 2018	[24]	4.0–2.0
Liu, Wang, et al. 2017	[25]	1.58–2.0
Lee, Joo, et al. 2014	[26]	0.6–1.8
Rosa-clot, Tina, et al. 2017	[5]	10
Yadav and Gupta. 2016	[27]	0.79
Azmi, Othman, et al. 2013	[18]	2.82-14.58
Majid, Ruslan, et al. 2014	[28]	5.93–15.5
Kamuyu, Lim, et al. 2018	[3]	14.69

Table 1.2: Comparison between ground-mounted PV and base- and proposed-concept FPV [15]

	Ground-Mounted PV	Base FPV	Proposed FPV
Energy production (GWh)	141.71	145.72	186.05
Annual insolation (kwh/m^2/day)	5.02	4.66	6.17

Around extra 10 % of the module efficiency can be easily gained by installing the PV module over the surface of water [5]. Furthermore, the annual energy yield $kWh/year$ can be increased with about 15 % by adding what's called "Water Veil", which allows the PV modules to remain at low temperatures during the hot weathers [5]. Figure 1.6 shows a layout of floating PV plant with a tracking system based on adding a water veil for the purpose of cooling the solar modules [6]. In [6] the author has derived an equation that relates directly between the electrical efficiency $\eta_{c,FPV}$ and the module temperature T_m and predicted that a 1 $°C$ increase in the module temperature results in a decrease of 0.058 % in the electrical efficiency, as shown in equation 1.1

$$\eta_{c_{(FPV)}} = 15.96 - 0.058T_m \tag{1.1}$$

Figure 1.4 shows the relation between the module temperature and the corresponding electrical efficiency of module. It also performs a comparison between two different Efficiency-Temperature models of the floating PV modules (Empirical and Calculated model). The empirical model by [3] has recorded an ideal efficiency of 14.69 % with a module temperature of 21.95 $°C$, while the calculated model by this study shows a PV module efficiency of 14.669 %. The efficiency deviation ($\Delta\eta$) between the two models is almost $\pm$0.15 %. For example

at a module temperature of $-3.831°$ C the calculated efficiency $\eta_{calc} = 16.016$ % while the empirical predicted efficiency is $\eta_{emp} = 16.182$ % while at a module temperature of $51.526°$ C the empirical and the calculated efficiency are 12.97 % and 13.124 % respectively as shown in table 1.3.

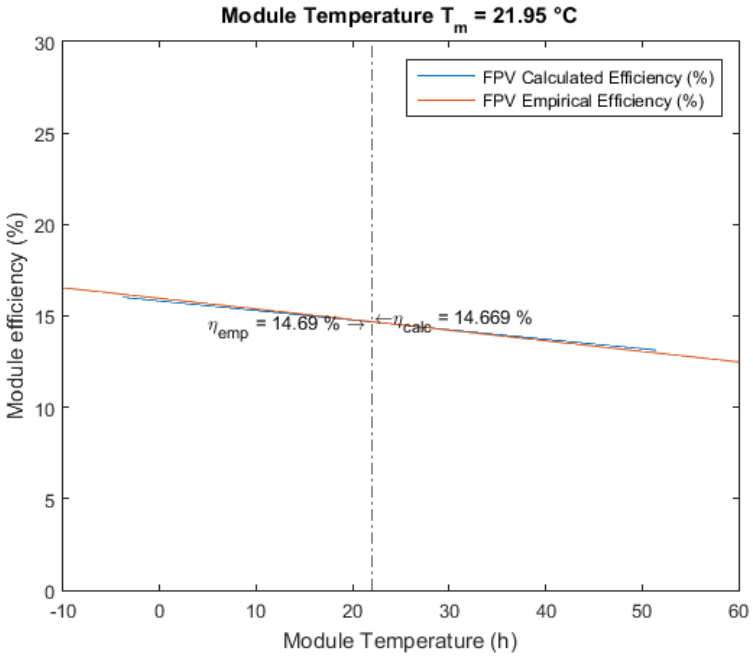

Figure 1.4: FPV module temperature versus the instantaneous electrical efficiency (A comparison between the predicted module efficiency by [3] and the efficiency calculated by this work)

Table 1.3: A comparison between the predicted module efficiency by [3] and the efficiency calculated by this work

Module temperature (° C)	$\eta_{emp}(\%)$	$\eta_{calc}(\%)$	$\Delta\eta(\%)$
-3.831	16.182	16.016	0.166
21.95	14.69	14.669	0.021
51.526	12.97	13.124	-0.154

1.4 Water Veil

The performance of the PV modules can be improved by decreasing the cell operating temperature which highly depends on the ambient and the PV module temperature. Reducing the thermal degradation of the PV modules can be reduced by cooling the outer surface of the PV module which results in a lower cell temperature as well as a better efficiency. One of the

proposed methods of cooling the upper surface of the PV module is called *Water Veil*, which is achieved by installing the water cooling in an irrigation system on the PV module. However, such kind of PV surface cooling can attain an increase of the output power of about 15 % [29]. Cooling of PV modules is necessary for two main reasons: to increase the lifespan of the PV cells and to increase the efficiency as well as to improve the performance of the PV cells. The cooling system is illustrated in figure 1.5. The main components of the system configuration are as follows:

1. Inlet water tube arrangement positioned on the top of the PV module (Irrigation pipes).
2. Water tank for storing the cold water (In case of FPV it is not required).
3. Conduit for collecting warm water.
4. Water pump.
5. A control system to control the water pump in case of higher temperature (For example more than 30° C).

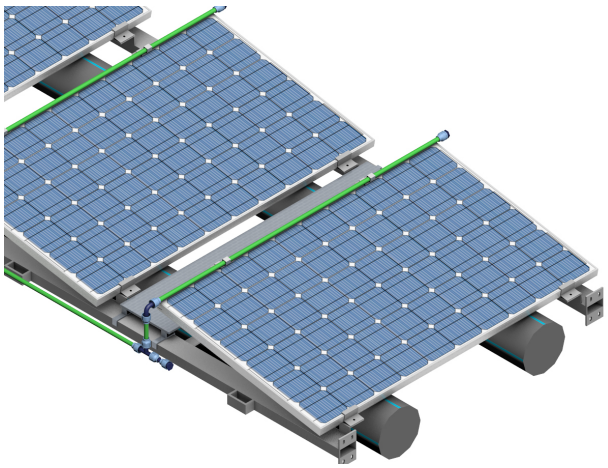

Figure 1.5: Water cooling configuration of PV modules (Water Veil) [4]

1.5 Solar tracking system

The photovoltaic systems can be distinguished into two main types: fixed-PV where the tilt and azimuth angles are adapted to harvest the highest portion of the solar irradiation but finally they are fixed, the other type is the tracking-PV where the tilt and azimuth angle can be changed over the whole day based on the location of the sun and namely the time. Since, the highest amount of energy from the sun can be collected when the solar ray is perpendicular to the surface of module. This function is done by adding real time sun tracker to the PV module. However, the electricity generated by the dual axis tracking PV is 30 % greater than the fixed PV.

The tracking-PV is designed before all to detect the position of the sun by using a solar sensor, which directly gives a feedback signal to the control system. Subsequently, the control

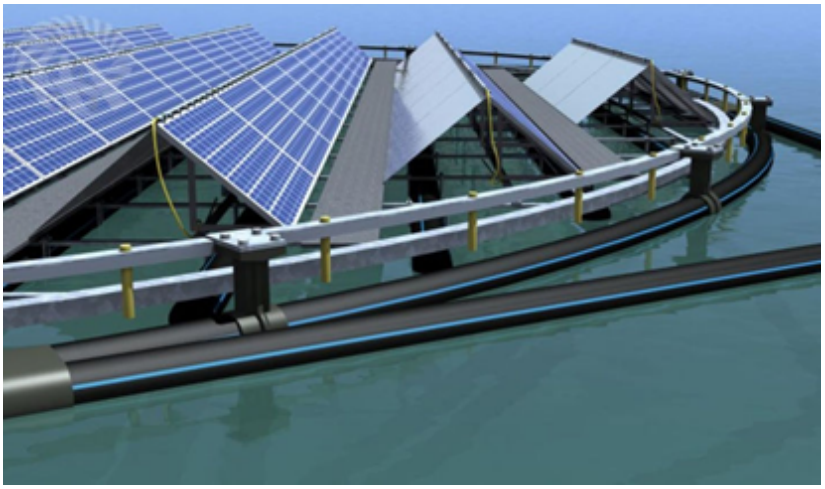

Figure 1.6: Layout of Floating tracking cooling concentrating (FTCC) [5]

system gives a control signal to the assigned motor to move the mechanism accordingly. The ground-mounted PV system has some limitations with respect to the single tracker, since PV modules that operate with the single tracker should be below 3 kW_p. Floating PV gives the advantage of more flexibility and freedom as the whole self-weights including the under-construction of module and the floaters are transferred directly to body of water through the buoyancy.

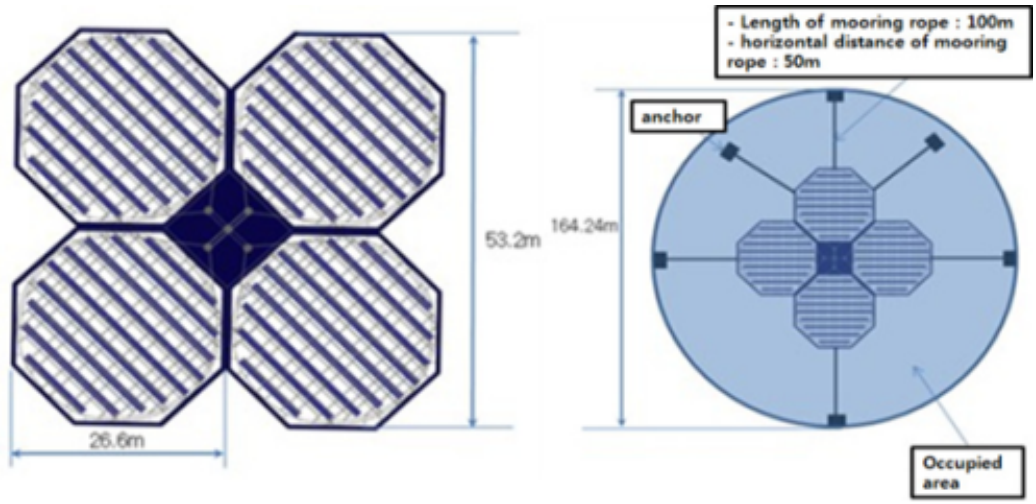

Figure 1.7: Floating PV-Tracking system [6]

Furthermore, the tracking system of FPV is relatively simpler than GPV, therefore, the malfunction will be reduced. Figure 1.7 shows the construction model of a floating photovoltaic tracking system that consists of a internal (moving) and external (fixed) structures. It will be discussed in detail later in chapter (Tracking FPV). Moreover, the FPV that is equipped by a tracking system has a relatively row costs than the tracking systems for GPV.

The ground-mounted PV (GPV) system has some limitations with respect to the single

tracker, since PV modules that operate with the single tracker should be below 3 kW_p. While the floating PV gives the advantage of more flexibility and freedom as the whole self-weights including the under-construction of module and the floaters are transferred directly to water through the buoyancy. Furthermore, the tracking system of FPV is relatively simpler than GPV, therefore, the malfunction will be reduced. Figure 1.9 shows the construction model of a floating photovoltaic tracking system that consists of a internal (moving) and external (fixed) structures. Moreover, the FPV that is equipped by a tracking system has a relatively lower costs than the tracking systems for GPV.

1.6 Ground reflection (ALBEDO)

The ground reflection factor (Albedo) can be well-defined as the amount of the solar irradiation reflected by a surface which is considered as a percentage of the total irradiation on the same surface. The reflected radiation back to the photovoltaic module can be calculated be equation 1.2. Where RTI is the reflected Tilted Radiation, GHI is the Global Horizontal Irradiation, ρ_A is the Albedo value and γ_M is the tilt angle of the module.

$$RTI = GHI \cdot \rho_A \cdot \frac{1}{2}(1 - \cos(\gamma_M)) \tag{1.2}$$

The performance of the PV module can be predicted by how much solar irradiation falls on surface of the PV module. However, on the large scale PV power plants the solar irradiation must be known previously in order to expect and calculate the generated energy form the plant later. Thus the climate data can be easily imported directly from one of the PV simulating software *(PV*Sol, PVsyst, Helios3D, SAM)* or directly downloaded from an open-source clime data provider like Photovoltaic Geographical Information System *(PVGIS)* or *(Global Solar Atlas)*. On the other hand a paid source for the world wide climate data *(Meteonorm)*. Nevertheless, when the climate data are not available for a specific site, another methodology is to perform an experimental data to create relations according to the air mass to calculate later the spectral correction coefficient [31]. Not only that, but also another technique is to generate a clear-sky spectra using a radiative transfer model tuned to the atmosphere of the location where modules are installed, and to utilize this spectra as a substitute for measured values [32].

In order to know how important Albedo calculations is for the solar module, it is must to recognize its effect on the module and namely on the output generated energy, as the improper prediction or calculation of the Albedo can lead to an error in the output power of module.

It is also clear as shown in Figure 1.8 that the Albedo ratio affects the output energy of a PV module significantly. Since the ratio of the Albedo irradiation to the in-plane irradiation (E_a/E_t) increases as the Albedo ratio increases [10]. In figure 1.8 it can be observed that the Albedo ratio dramatically affects the output energy out of the 90° module and less affects the 40° module. However, in reality, Albedo values are continuously changing based on the atmospheric conditions. In the Floating Power Plants (FPV), Albedo ratio should be considered while predicting the yield of the plant in advance, since there is an extra amount of the solar irradiation reflected by the surface of water and received by the PV modules. This amount of reflected irradiation depends significantly on the spectral nature of the water surface in addition to the inclination of surface with respect to the horizontal plane. Table 1.5 expresses

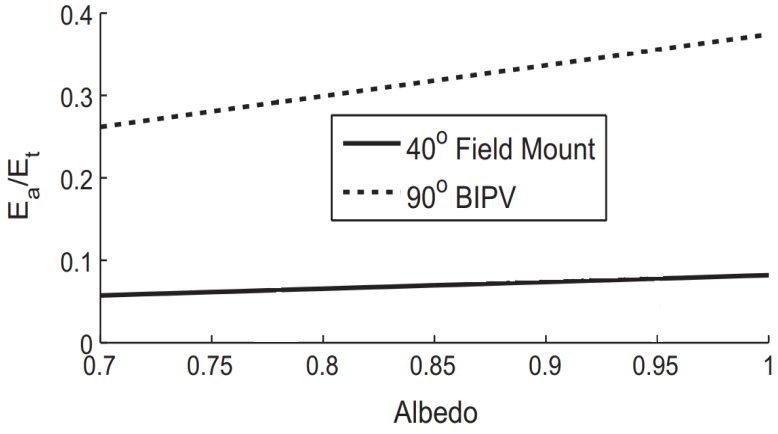

Figure 1.8: Effect of the Albedo ration on the performance of PV modules for both normal ground-mounted PV moduel tilted with 40° and Building-Integrated PV module (BIPV) tilted with 90° [10]

some Albedo values of for various ground natures.

The Albedo value describes how good the surface can reflect the solar radiation. In other words, it indicates to the "Whiteness" of the surface, since the white color is a good reflector of radiation and the dark colors absorb more solar radiation. An Albedo with 0 % means that the surface is completely dark and absorbs all solar radiation, while a value of 100 % indicates to a perfect reflective surface. As a result, the snow and sea ice have higher Albedo values compare to the liquid water. For example, the sea ice has 30 % - 40 % while the thick sea ice covered with whether fresh and old snow has an Albedo value up to 90 %. On the other hand, the ratio of Albedo falls between $3-22$ % in case of rivers, lakes or normal water surfaces [16]. In practice, in the northern areas the Albedo values are underestimated in winter and overestimated in summer. For reaching the highest yield out of the PV module, it is recommended to install the PV modules with the consideration of a changeable tilt angle for a high average yield over the entire year.

Table 1.4: A comparison between the usage Mono- and Bi-Facial PV modules to show the specific annual yield for each of them for a 100 kW_p FPV [PV*Sol]

Cell technology	Mono-facial	Bi-facial	Difference (+/-)
Global Radiation at the Module (kWh/m^2)	217.01	239.06	+22.05
Specific Annual Yield (kWh/kW_p)	1,143.92	1,207.76	+63.84
PV Generator Energy ($kWh/year$)	114,346	120.727	+6,381
Required area (m^2/kW_p)	5.26	5.05	+0.21

In addition, for a better harvesting of the solar irradiation with respect to the ground reflection, BI-facial PV modules can also be a good choice. For clarifying this point, an FPV power plant has been simulated using (PV*Sol) Table 1.4 shows how better the usage of Bi-

facial PV module than the Mono-facial one is, as the specific annual yield for a 100 kW_p FPV plant is $1,207.76$ kWh/kW_p and $1,143.92$ kWh/kW_p for Bi- and Mono-facial PV modules respectively.

Although the presence of a PV plant in snow area would be beneficial for higher harvesting of energy not only because of the ground reflection but also because of the low ambient temperature, but It is also important to take into consideration the losses due to the snow. Since the during the winter seasons the snow mask the PV module surface and reduce the direct irradiation falling on it. However, in the clear weather periods the energy production will be of course greater than other periods, therefore, in the very earlier stages both Albedo ratio and also the losses due to snowfall must be taken into consideration for better prediction of the yield.

Table 1.5: Typical estimated values of Albedo [16] updated by [17]

Surfaces	**Albedo (%)**
Water in low sunlight	50 – 80
Water surface (angle of inclination > 10°)	22
Water surface (angle of inclination > 20°)	12
Water surface (angle of inclination > 30°)	8
Rivers and lakes	5 – 10
Sea	3 – 8
Fresh snow	90
Old snow	45 – 90
Glaciers	20 – 45
Sea ice	30 – 40
Sandy ground	20 – 40
Dry sand and dunes	25 – 45
Rock (cliffs)	10 – 40
Veldt	20 – 30
Forest	5 – 20
Dark soil (e.g. brown earth)	10 – 20
Grassland, agricultural crops	10 – 25
Uncultivated fields	26
Lawn	18 - 23
Residential areas	15 - 20
Cropland	5 – 20
Asphalt	15

1.7 Reflector possibility

One of the advantages of the tracking systems is the possibility of adding a reflector over both sides of the solar module. This allows more harvesting of energy by means of some aluminum concentrators. However, the modules are installed with the optimum tilt and azimuth angles to gather the highest irradiation. Sometimes, the shadows cannot unfortunately be compensated, since there may be some trees and chimneys near to the modules. Therefore, the reflector compensates the losses due to the partial or complete shadowing of module. Shadows can also be caused due to the less spacing between the module rows since the front-end modules can shade the back-end modules.

Accordingly, an appreciated spacing “Catwalk” between module rows must be considered. Such a simulation can be easily done in advance and before the erection of the PV plant by one of the modeling software like “PV*Sol”, which allows the user to simulate the shadowing whether on the solar module or around it. However, these software perform the shadowing simulation based on the “MeteoSyn”, which is a huge location-dependent database for the climate data such as air temperature, wind and solar irradiation.

A solution is proposed in [7] is to add reflectors on both sides of the PV modules which are inclined with 2° as shown in figure 1.9. The amount of the reflected solar irradiation depends on the reflector angle as well as the correct alignment.

Figure 1.9: Floating PV with reflector "V-trough" solution [7]

Chapter 2

Moisture ingress into Photovoltaic modules

Encapsulant materials are normally used for sealing the PV module after the integration and soldering of the solar cells together into the module. Generally, two layers of encapsulate material (e.g. Ethylene-Vinyl-Acetate - EVA) are used to sandwich and wrap the silicon cells. It is relatively cheaper. However, it must not only provide a perfect sealing for the cells but also a high adherence with both the outer glass sheet and with the back-sheet (lower layer). Because the PV modules are supposed to operate reliably for 25 – 30 years they must be able to withstand the stressful abnormal conditions such as storms, moisture, temperature, humidity, etc. Furthermore, EVA materials must enable a very high transmittance to gather as high irradiation as possible and the resistivity to the UV radiation.

The ingress of water into a PV module affects the performance significantly. The corrosion rates are continuously increasing when the moisture infiltrate the module [9], and this occurs because of the poor sealing of the PV module. Therefore, the degradation and failure rates of the module become higher, as a result the lifespan of module would be absolutely decreased. The cover glass alone is incompetent to prevent the ingress of water as well as the moisture from the whole edges of the solar module for up to 30 years lifespan. The encapsulation materials must be previously determined whether it can protect the module against the ingress of water and moisture. Nowadays, some of Thin film based solar modules are considered as less expensive than the traditional silicon-based ones but the must demand a superior grade of protection against the environment stresses.

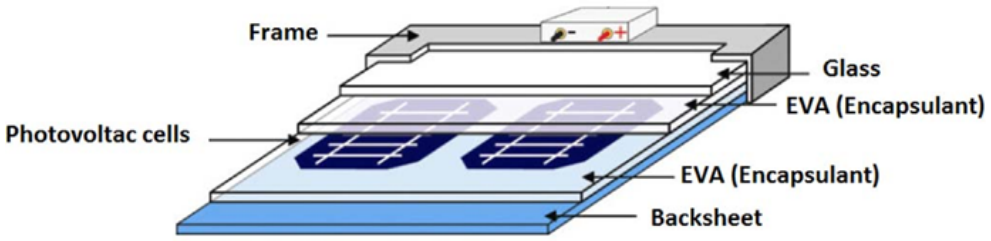

Figure 2.1: The components of a solar PV module [9]

Although some photovoltaic modules are fabricated with impermeable front- and back-sheets, as they will offer a good diffusion of the moisture across the edges of the solar module, they cannot completely protect against the ingress of moisture for 20 – 30 years lifetime as water can also permeate into the module, which causes later the corrosion. Therefore, there are nowadays what is called (Breathable) composition of the photovoltaic module, with the help of such kind of technology, the modules are allowed to be easily dried out during the whole sunny day [9].

Consequently, the diffusivity of water into a photovoltaic module must be previously measured and verified, not only that, but also the absorption capacity of EVA material should also be specified for obtaining a right water ingress model. Such processes are done in order that we can determine the time in which the module comes into equilibrium after facing the environmental effects.

2.1 Ingress protection (IP index)

As the floating power plant may be installed directly offshore or near-shore, the electrical and electronic components and equipment must withstand hazards and weather conditions. In particular, the transformer station, Inverters enclosures, standby generators (For hybrid FPV), electrical rooms, electrical cables, cable lugs and glands. The International Electrical Commissioning [8] has classified the protection provided by the enclosures given by an electrical equipment a rated voltage not more than 72.5 kV as the following:

- Protection of persons inside the enclosure against any hazards.
- Protection of electrical components against solid foreign objects inside the enclosure.
- Protection of electrical components against the dangerous effects due to ingress of water.

Also, the electrical equipment inside enclosures should be well protected against the external abnormal conditions such as:

1. Moisture
2. Corrosion
3. Explosive materials
4. Overheating
5. Icing
6. Operating fans outside the enclosure

Figure 2.2 expresses the elements of the IP index of protection and how it can be read. For example, $IP21$ means that the electrical equipment must not allow a human finger as well as solid objects with a diameter more than 12.5 mm to pass through it and a protection against the vertical dripping of water. On the other hand, $IP76$ means a complete electrical protection against the dust and the access of hazardous parts like wires in addition to the temporary immersion of the electrical equipment into the water.

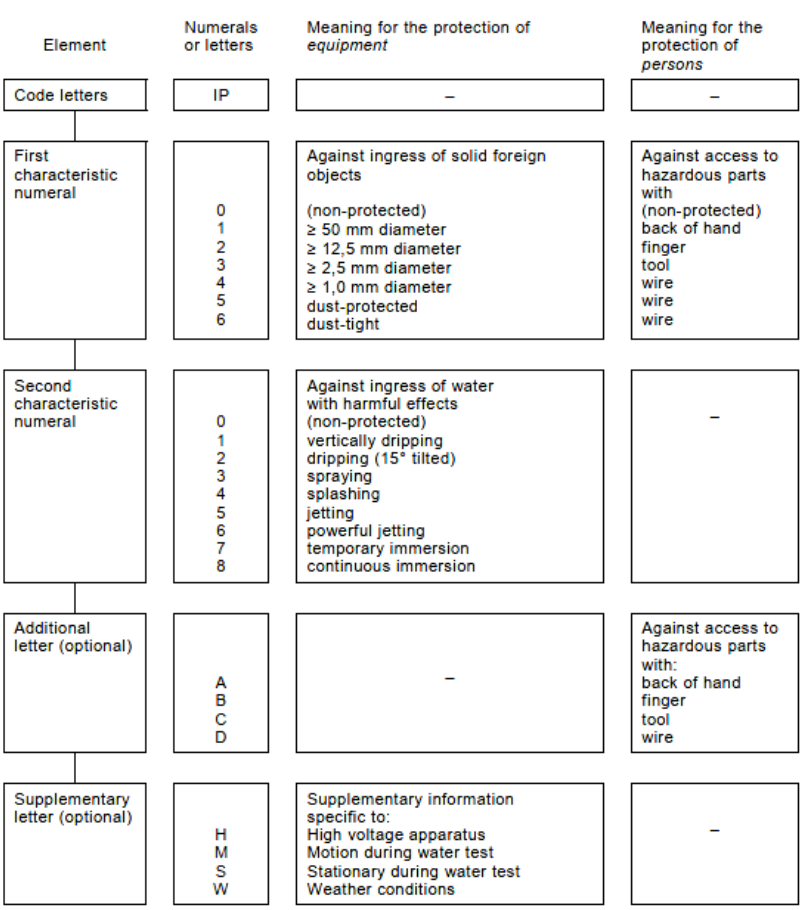

Element	Numerals or letters	Meaning for the protection of *equipment*	Meaning for the protection of *persons*
Code letters	IP	–	–
First characteristic numeral	0 1 2 3 4 5 6	Against ingress of solid foreign objects (non-protected) ≥ 50 mm diameter ≥ 12,5 mm diameter ≥ 2,5 mm diameter ≥ 1,0 mm diameter dust-protected dust-tight	Against access to hazardous parts with (non-protected) back of hand finger tool wire wire wire
Second characteristic numeral	0 1 2 3 4 5 6 7 8	Against ingress of water with harmful effects (non-protected) vertically dripping dripping (15° tilted) spraying splashing jetting powerful jetting temporary immersion continuous immersion	–
Additional letter (optional)	A B C D	–	Against access to hazardous parts with: back of hand finger tool wire
Supplementary letter (optional)	H M S W	Supplementary information specific to: High voltage apparatus Motion during water test Stationary during water test Weather conditions	–

Figure 2.2: Ingress Protection Index (IP) Meaning of each letter [8]

Furthermore, there are additional letters which may be also added to the IP protection index, and also can be omitted without replacement. For example, the letter A means that the equipment is protected against the access with the back of hand and C means protection of tool. Besides that, the letter M means that the equipment is tested for the harmful effects because of the motion of moving parts under-water (For example, the rotor of an electric machine), while the letter S means that the equipment is tested against the hazards which are affected by moving parts under-water (For example the rotor of an electric machines) but in a stationary condition.

2.2 Forms of IP code

The IP code can be written in many forms. The following examples expresses the arrangement of numbers and letters in IP code;

IP76 - no letters

IPX4 - omitting the first number

IP2X - omitting the second number

IP30A - keep the two numerals and adding an additional letter

IPXXH - omitting both numbers and adding an additional letter

IPX2C - omitting the first number, and addition an additional letter

IP2XS - omitting the second number, and addition an additional letter

IP21CM - adding both the additional and the supplementary letters

IPX5/IPX6 - equip the electrical equipment with two different protection degrees

2.3 The protection against the access of hazardous materials and tools expressed by an additional letter

The additional letters are used to express the protection against the access of foreign hazardous tools or parts, table 2.1 shows the meaning of each letter [8]. The additional letters are are used in the IP code only;

- if the current protection against the hazardous parts is already greater than the one expressed by the first number.
- if the degree of protection against the hazardous parts is already expressed on the enclosure, in this case the first number is omitted and replaced by **x**.

Table 2.1: The meaning of the additional letter added to the IP protection code

Additional letter	Head description	Definition
A	Protection against access of the back-hand	Protection against a foreign solid object with a 50 mm ϕ
B	Protection against access of a human finger	Protection against access of a solid object with a 25 mm ϕ and 80 mm length
C	Protection against access of a tool	Protection against access of a solid object with a 12.5 mm ϕ and 100 mm length
D	Protection against access of a wire	Protection against access of a solid object 1.0 mm ϕ and 100 mm length

According to (Solar Energy Research Institute of Singapore) -SERIS, the floating based inverters must have an Ingress Protection index (IP) not less $IP67$ so that it could deal with the effect of the moisture. Furthermore, it would be highly recommended to erect the inverters on land if the distance is not too great. Regarding the cables (In the case of cabling, we are having a second look. it is observed that the cables in a few sections in our test bed lead to lower insulation resistances, which in turn cause the inverters to temporarily not connect the array for safety reasons, i.e. due to suspected leakage currents) [30].

Chapter 3

How do the characteristics of PV change due to the variation of temperature?

The operating solar cell temperature T_c is playing a very important role during the operation of the photovoltaic module, since both the electrical efficiency as well as the output power are strongly affected by the variation of the operating temperature, which is determined afterwards by the energy balance of the solar module. Once the solar radiation falls against the solar module some of it will be already absorbed and converted into two forms of energies: thermal and electrical. The rest of the solar radiation will be reflected to the atmosphere. However, the operating temperature of the solar cells should be reduced as much as it can be in order to obtain the best performance from the PV module.

In order to distinguish between the ground mounted PV and the Floating PV, a detailed simulation model of the cell operating temperature versus the output power and the instantaneous efficiency per unit time must be performed. The cell temperature may be influenced by the cooling effect of water, when the module is installed over the water surface as for the floating power plants.

In practice, the electrical performance of the PV modules is influenced also by the solar cell type. The common used the silicon-based solar cells technologies nowadays are a-Si and Si. As the efficiency of crystalline silicon increases as the output power of the solar module also increases. Additionally, higher temperatures result in lower efficiency of the module, in addition to a lower performance. The output power can be predicted by using the temperature factors which are expressed by the PV module's manufacturer and also differ from a module to another. Normally, the temperature coefficients are stated according to the Standard Test Condition (STC) [1000 W/m^2, 25 $°C$, 1.5 AM]. However, those coefficients are typically expressed in ($\%/K$). For example, if a solar module has a temperature coefficient of -0.5 $\%/K$, that means the output power will decrease by half percent for every degree of temperature above 25 $°C$ (298.15 K).

3.1 Voltage (V)

Although the temperature coefficient looks small, but the significant impact of the temperature rise can easily be shown in the hot weather areas. The voltage and the current are also changing repeatedly according to the operating temperature. The instantaneous voltage of the PV module can be determined by equation 3.1. For instance, the voltage decreases as the temperature increases, for example if a module has an open circuit voltage ($V_{oc}(T_1) = 21.06\ V$) and a voltage temperature coefficient β of $-0.27\ \%/K$, that means the open circuit voltage will decreases when the cell temperature increases to 35 $°C$ the voltage will decrease to ($V_{oc}(T_2) = 20.49\ V$). On the other hand, when the temperature becomes below than 25 $°C$ for example 10 $°C$ the voltage will then increase and become ($V_{oc}(T_3) = 20.87\ V$). Figure 3.1a shows how the voltage is influenced and changed according to the change of the temperature.

Figure 3.1 shows an example of a solar cell, which has an open circuit voltage of 20.06 V at the Standard Test Conditions (STC). It is also clear that, as the temperature increases the I-V curve is shifted to the left-hand side, as also the voltage decreases. Likewise, when the temperature decreases the curve is shifted towards the right-hand side as the voltage increases.

In practice, the voltage is affected significantly by the temperature change more than the current. Since the current is less affected by the change in temperature as the whole curves are nearly above each other.

$$V_{oc(T)} = V_{oc,STC}[1 + \beta(T - T_{STC})] \tag{3.1}$$

The effect of the temperature on the voltage becomes quite significant for the low power consumption PV products. For example, a solar energy powered mobile charger, which is uses a buck converter for reducing the input voltage out of the PV module down to mostly 5 V in order to be suitable for the mobile phone battery.

Those kinds of products are facing a great problem during the low radiation or very high temperature periods. For instance, at a high temperature the output voltage of PV module becomes low. Therefore, the output voltage of the Buck converter also becomes low and unfortunately cannot match the requirements of the phone battery. Furthermore, if the Buck converter circuit does not have a protection diode there may be a reverse current from the phone battery back to the solar module which may damage it as it becomes in this case a load. On the other hand, for the large-scale power plants a change in the operating voltage due to the temperature variation means the change of the operating point. Normally, the photovoltaic power plants are operating on the Maximum Power Point (MPP) which achieves the maximum operating performance of modules otherwise the module will not operate efficiently. Similarly, the current will also be concerned by the change of the cell temperature since it increases a little bit by the rise of the temperature. Although this is not considered as a strike change, but the maximum power point will be changed accordingly.

3.2 Current (A)

Similarly, the current is also influenced by the cell- and the ambient-temperatures variation, although it seems that it is not much affected. This also can be easily realized by the small

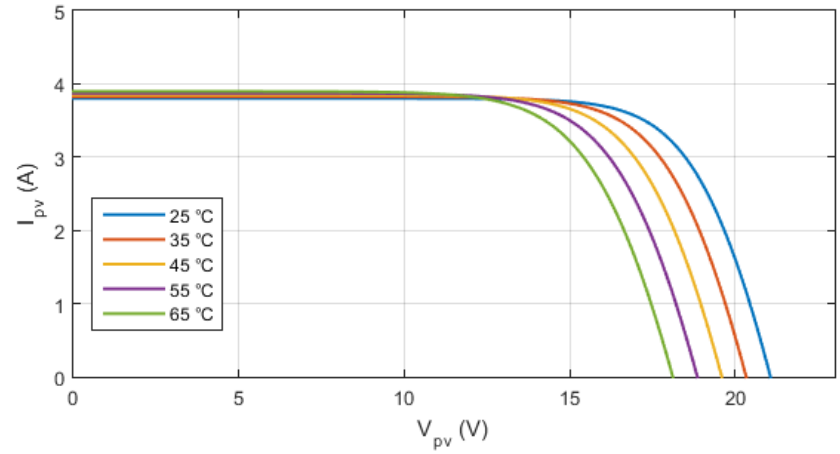

(a)

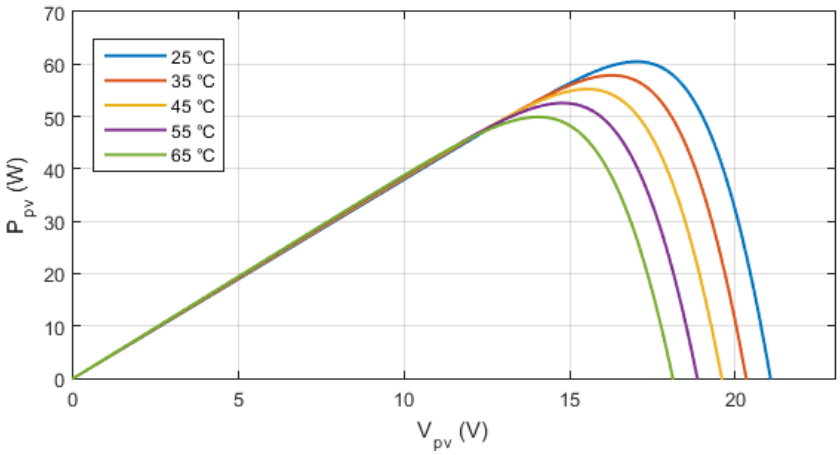

(b)

Figure 3.1: (a) Solar cell I-V curve (b) Solar cell P-V curve with different temperatures

amount of the current-temperature coefficient. Not only that, but also the temperature coefficient of the cell current must be always positive, since the current is inversely proportional to the cell temperature. For example (according to equation 3.2), if a solar cell has a current temperature coefficient of $[+0.04\ \%/°K]$ and a standard short circuit current of 3.80 A ($I_{SC} = 3.80\ A$) that means when the cell temperature increases to e.g. 35° C then the short circuit current count to 3.815 A. Similarly, when the temperature increases again to 65° C then the short circuit current will also increase to 3.86 A. See Figure 3.1a.

$$I_{sc(T)} = I_{sc,STC}[1 + \alpha(T - T_{STC})] \tag{3.2}$$

3.3 Power (W_p)

The output power of the solar PV module is the product of voltage and current. Since both the voltage and current have been changed due to the variation of the temperature, the output

power shall also accordingly change. Figure 3.1b shows the (P-V) characteristic curve of PV module with various temperatures and fixed radiation (1000 W/m^2). Figure 3.1b presents the relation between cell voltage and power at the STC temperature ($T_c = 25\ °C$) – Blue curve – as well as different temperatures. Furthermore, the maximum power point position on the curve is always changing according to the change of operating temperature and voltage. Consequently, operating the PV module under a relatively low temperatures is good for harvesting much power out of the PV module as for the floating PV power plants. Table 3.1 shows a comparison between the normal mounted PV module versus the FPV module with respect to the output power and the corresponding efficiency due to the variation of the temperature.

Table 3.1: Output power, electrical efficiency and the average PV module temperature at a solar irradiation of 834 W/m^2 [18]

	PV	FPV	PV	FPV	PV	FPV
Temperature (T_{av})	36.6 $°C$	34.8 $°C$	56.9 $°C$	52.8 $°C$	66.2 $°C$	60.6 $°C$
Power (P_{max})	4.87 W	5.41 W	4.17 W	4.87 W	4.10 W	4.8 W
Efficiency (η_{elec})	5.31 %	5.90 %	4.55 %	5.31 %	4.47 %	5.23 %

3.4 PV modules cooling techniques

As discussed in chapter 4, the performance of the FPV module is primarily influenced by the temperature, as the output power as well as the electrical efficiency increase as the temperature decreases. Thus, another feature was additionally suggested in order to keep the advantages of the floating PV and to increase the cooling effect so that the FPV performance becomes also higher.

The various cooling techniques are used for lowering the PV modules temperature. According to the size and shape of the PV plant, the type of cooling system is chosen. Generally, the cooling systems are classified into two main types; Active and passive techniques. The passive cooling technique depends on the natural motion and circulation of air between the backside of PV modules and the surface of roof (In case of the parallel erection of PV modules on a roof see figure 3.2 and 3.3). Therefore, an appropriate spacing (Air gap) between the module and the roof surface must be taken into consideration. The passive cooling technique demonstrated to lower the temperature from 77 $°C$ to 39 $°C$ [33].

Another passive cooling technique was also introduced demands for some heat sinks attached along the back-side of the PV module and due to the conduction process, the heat energy transfers from PV module to the heat sinks. Such passive cooling technology has some limitations because the installed heat sinks makes the PV modules heavier as a result the costs also increase.

However, for the active cooling technique of floating PV a water irrigation system integrated to lower the temperature of PV modules using the heat transfer processes. Additionally it provides a low cost cooling-technique solution [34]. It consists of three main sub-systems;

1. A series of polyethylene pipes fixed on the top of the PV modules.
2. A pressurized pumping system which is responsible for pumping the water inside the pipes.
3. A control system to operate the water pump in the event of high temperature of PV panels (For example 30 $°C$).

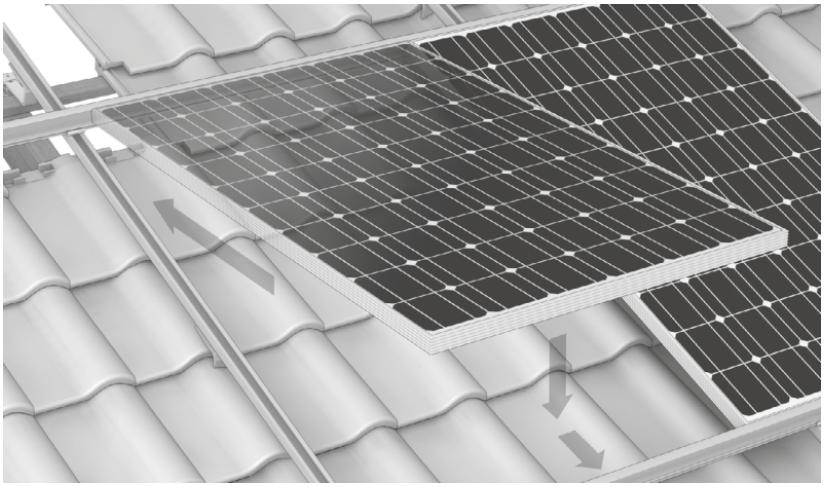

Figure 3.2: Roof-top PV mounting system [11]

Figure 3.3: Roof-top PV mounting system [12]

In the event of higher temperature of FPV modules, the control system trigger a control signal to the water pump to turn on based on the feedback-sensors measurements as shown in figure 3.4 [13]. Thus, the sprinklers operate and spray the cold water on the surface of PV modules to cool them down. In the suggested system in [13], water is stored in a tank which can be kept in the ambient temperature or to be buried under an appropriate depth to keep the water at low temperature. In case of FPV, water can be take directly from the water-body where the floating PV plant is erected without the need of integrating a water tank. Furthermore, back-water is accumulated down from the surface of PV module at the bottom of modules by using **"Gutters"** (See figure 3.5) [13].

However, water is pumped into the pipes which are installed along the PV modules at low temperature, pressure and speed using valves and sprinklers. In the end, during the accumulation of water, in order to avoid the soiling and the presence of microfilm in water, a filter is used to filter the back-water before re-pump it again in the pipes, which may damage or over-load the water pump. The water spraying can decrease the module operating temperature from 23 $°C$ to 5 $°C$ [35].

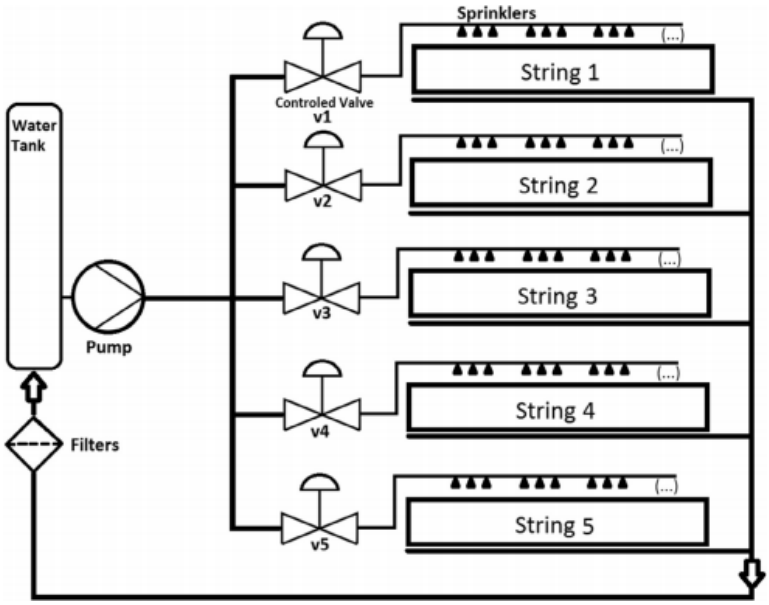

Figure 3.4: The schematic diagram of active water-cooling technique of cooling down the PV modules [13]

The supply of water at a constant low temperature is the most important factor of the system. Another water cooling technique called "Water Veil" can also be used for cooling down the PV modules by means of a thin layer of water on the front surface of PV module. Figure 3.6 illustrates an artistic view of the FPV power plant operated with water veil, as FPV modules are positioned in the center of the water veil floating ring, which is settled down from the sides on the floaters to be well-stabilized.

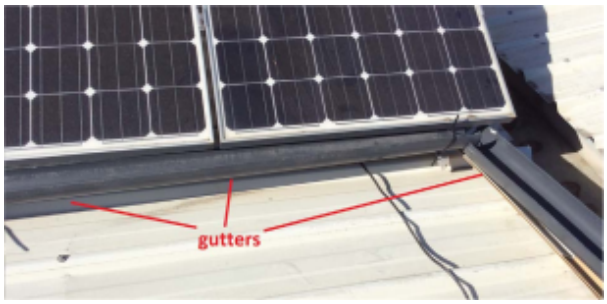

Figure 3.5: Way of accumulating water at the bottom of PV modules [13]

The water veil is few millimeters thick and integrated with a number of small valves to

distribute a water layer over the front surface of PV modules the whole day. The water-veil cooling technique does not only cool down the PV modules but also clean them, as the dust particles themselves reduce the solar irradiation coming toward the PV modules, which is worth it in the deserts and dusty areas. It was stated that the water-veil tend to an increase of output power from 8 to 12 % excluding the power driven by the water pump [35].

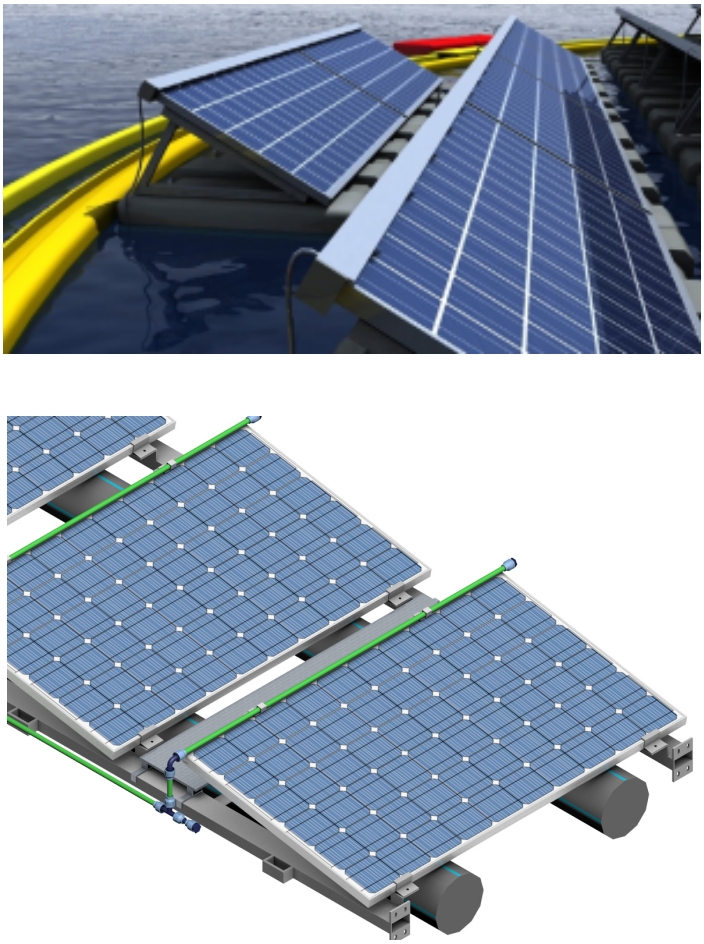

Figure 3.6: An artistic view of FPV power plant integrated with Water Veil cooling technique [5]

Chapter 4

Energy Balance

The electrical generated energy by the PV module depend significantly on the solar irradiation as well as the ambient temperature. Despite that, the global irradiation that is coming from the sun is not completely absorbed by the module accordingly the electrical energy will be also much lower. As discussed in chapter 3, as the cell temperature increases as also the output yield of the solar module decreases. Part of the solar irradiation is reflected back from the surface of the solar module and the rest continues through the front glass passing through the encapsulate material (EVA) and finally to the solar cells. In Practice, it is considered that the reflective losses of the solar irradiation are about 10 % of the whole irradiation [36]. The majority of the irradiation unfortunately generates heat and only the rest of it is used for generating electricity by the PV module. The whole output energy yield out of the PV module can be determined by the PV module efficiency itself. For instance, the typical efficiency of a-Si solar cells is 5 - 10 %.

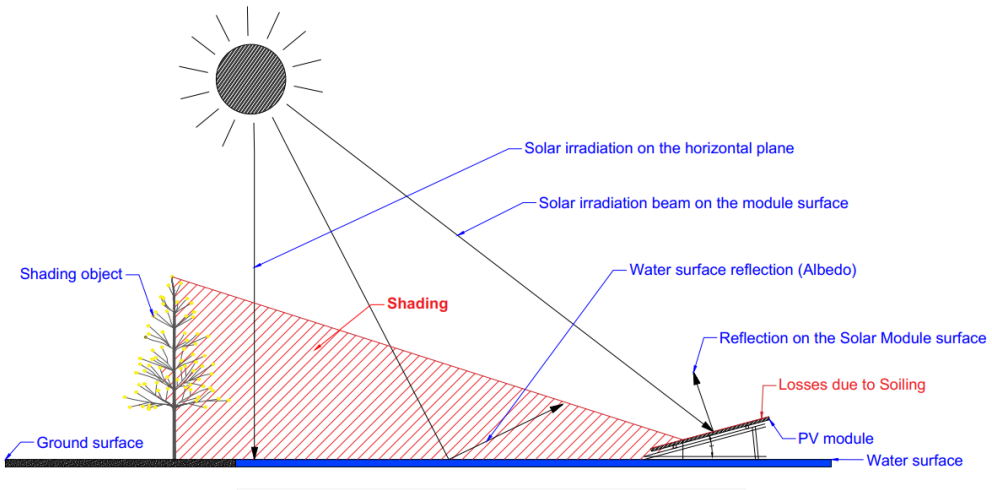

Figure 4.1: Solar radiation components and the factors that are influencing the output energy of a PV module as well as the solar spectrum

In practice, the solar irradiation absorbed and the harvested energy out of the PV module are also influenced some other factors, which are important in the earlier phases during the

prediction of the annual energy yield and for the simulation of the PV power plant before the erection stage. They are namely as the following:

- The deviation from the standard spectrum.
- Ground reflection (Albedo) as discussed in Section 1.6.
- Orientation and the tilt (Inclination) angle of the PV module.
- Cooling effect (Floating PV power plants).
- Shading (Mutual -The shading which is caused because of the small distance between the PV rows- or general -Trees, Birds etc.-).
- Reflection on the PV module front glass surface which particularly depends on the tilt angle of module and the material properties of the front glass.
- Soiling or the covering of snow on the front surface of PV module.
- Solar cell efficiency which is continuously changing based on the cell temperature, which also depends on the surrounding ambient temperature.
- Electrical losses.

4.1 Deviation from the standard spectrum

The efficiency of the PV module is significantly influenced by the variation of the solar spectrum. Moreover, the standard nominal value of the solar module stated previously by the manufacturer is measured in the Standard Test Conditions (STC). In other words, under the consideration of solar irradiation of 1000 W/m^2 IEC-60904-3 [37]. Since the standard solar radiation spectrum not constant over the time, the output power and the performance of PV modules will accordingly deviate from the nominal values. These values can also be predicted in advance based on the location of the PV power plant as well as the ambient temperature. However, the climate data considered in this work is downloaded from ***Meteonorm*** and the location is ***"Auf dem Maiwald-See im baden-württembergischen Renchen, Germany"***. The results of the solar irradiation values were taken every one hour in a single year 2005. For the given location and the specified year, it was investigated that, there is a significant variation of the solar spectrum over the entire year which impacts the PV module performance ratio.

Since the instantaneous solar spectrum is different from the standard one at for a given location and time, the effective irradiation must be determined for getting best results of output power prediction, it can be calculated using the following equation:

$$G_{eff} = G \cdot \frac{\int S_r(\lambda) R(\lambda) d\lambda}{\int S_r(\lambda) R_{STC}(\lambda) d\lambda} \tag{4.1}$$

Where, $R(\lambda)$ is the solar light spectrum which is also different from the standard spectrum $R_{STC}(\lambda)$, and $S_r(\lambda)$ is the spectral response of the investigated PV module.

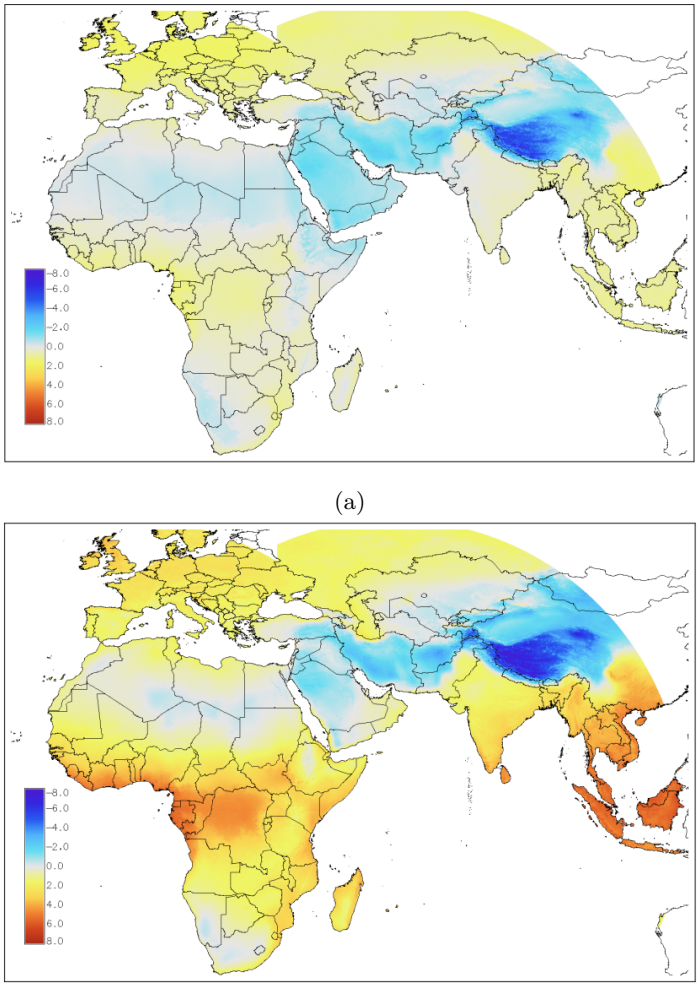

(a)

(b)

Figure 4.2: The relative deviation values from the standard spectrum in (%), the effective radiation is always taken proportional to the STC irradiation. (a) Deviation percentages for c-Si solar cells (b) Deviation percentages for CdTe solar cells [14]

Therefore, when the irradiation spectrum is different from the standard spectrum G_{eff} must be determined and considered later for calculating the annual output power of the PV module. As a result, the G_{eff} will replace the general spectral irradiation G during the calculation of the PV module performance [14].

The efficiency of the module is determined for each value of the solar irradiation, so that the performance can be calculated later with the thoughtfulness of the instant ambient and cell temperatures. Figure 4.2 shows that, the standard deviation values from the solar spectrum is everywhere less than one percent, while in some locations less than 0.5 %. In practice, the deviation from the standard spectrum of solar radiation is taken 1 %, although this is not an accurate value and the performance may of course change.

The output relative power of the PV module can be determined based on the incident irradiation and the ambient temperature. In practice, a mathematical model is used for predicting

the performance of the PV module which is described in [38]. In practice, the investigations from this model has proved that, the model can work successfully for various technologies of solar cells and the results from it were satisfactory [38]. The model can be expressed as equation 4.26.

In practice, the output power of module should be determined for each instantaneous value of the irradiation in order to investigate the how much the performance is influenced by the change in the irradiation as well as the ambient temperature. However, the calculations were done on the PV module which is installed over the surface of water over the whole year 2005 in each hour. As a result, the output power is not constant but changes significantly over the time based on the ambient conditions and irradiation. For example, a mono-facial PV module with 350 W_p was studied. Furthermore, it is noted that, the calculated output power of module may be greater than the nominal power (In this case 350 W_p), this is because of the lower temperature in the chosen location (Renchen, Germany). Not only that, but also, sometimes the calculations showed very lower values of the power due to the raise in temperature over the STC and/or the lower irradiation value. Nevertheless, in table 4.3 there are different values of the PV module power versus the ambient and the cell temperature, the time of the year, and the instant irradiation.

4.2 Ground reflection (Albedo)

The ground reflection plays an important role in the calculation of the performance of PV power plants. Since there is an amount of the irradiation that is reflected back from a surface to the surrounding ambient. In practice, it is considered with high effect when Bi-facial PV modules are used instead of the Mono-facial as they can react to the direct incoming radiation by the front surface as well as the back surface also. For example, if we erect some PV module on the surface of water (With an angle of inclination of greater than 10°), therefore, the Albedo value is supposed to be 22 % (See table 1.5). As a result, about 22 % of the solar irradiation will be reflected back towards the PV module back-surface because of the surface of water. Figure 4.3 shows how the bi-facial PV module look from both sides.

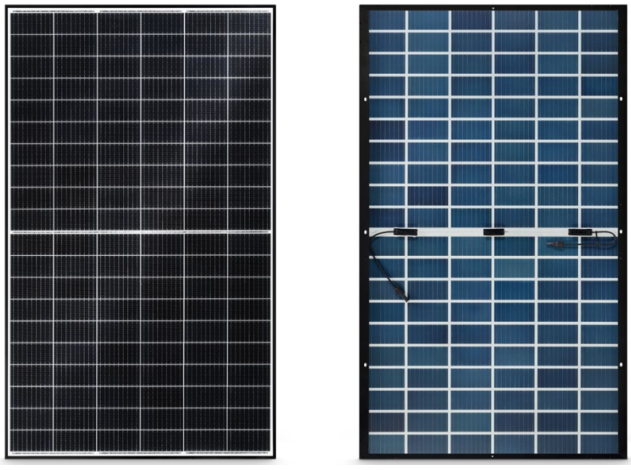

Figure 4.3: [Left] Front-side [Right] Back-side of Bifacial PV module [SOLON, R-WG 120n]

The amount of heat losses are not only affected by ambient conditions but also by the module materials. However, nowadays there are many conducted researches on how to improve the solar modules material quality in order to harvest the highest amount of solar irradiation. There are three main forms of heat losses which present in the solar module modeling; Conduction, convection, and radiation.

4.3 Thermal modeling of the PV module

The thermal modeling of PV module is considered of high importance in order to determine the cell operating temperature over a period of time, as a result to predict the output power of the module. The object of such simulation is to optimize both the electrical and the thermal performance of PV modules. In particular, a Capacitor/Resistor (RC) (As losses components) thermal model is to be performed in order to calculate exactly the thermal losses of the PV module. For instance, the thermal model expresses the instant temperature at each point within the PV module, which allows later to predict the heat flow with the module.

In particular, temperature rise before the operation, during the start-up, and during the actual operation of module can be easily determined for higher accuracy calculation of thermal energy losses. However, the temperature rise not only reduces the module efficiency, but also, can cause what's called **hotspot** which of course shortens the lifetime of the PV module and in some cases damages the module solar cells when the module is not protected against it. Consequently, a thermal modeling of the PV module must be carried out in advance for a given location and climate data in order to avoid the efficiency reduction of the damage PV module.

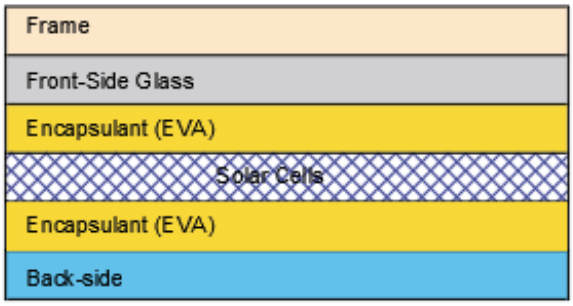

Figure 4.4: PV module anatomy

A thermal modeling method of PV module with DC-DC converter is performed [39]. It allows the quick prediction of the temperature within a PV module which is a DC-DC converter attached to the back-side. However, this thermal model introduced a useful straight-forward way to integrate a DC-DC converter onto the PV module.

Furthermore, another thermal analysis method is realized in [40]. In this model a thermal modeling is performed of a Concentrating Photovoltaic (CPV). In particular, a thermocouples are used for understanding the heat exchange and dissipation within the PV module. Moreover, some of thermocouples are placed inside the PV module as well as outside it, in addition to that, the analysis were done for both indoor and outdoor conditions.

In order to understand the heat flow within a solar module, three main thermal processes must be clarified well. In practice, when the PV module is placed in the atmosphere, not all of the irradiation is converted into an electrical energy, but some of it is lost as a form of heat losses. The PV module exchanges heat with the surrounding atmosphere where the module is placed. Heat exchanges through; Conduction, Convection, and Radiation. Furthermore, the other electrical components which are installed in the PV system are also generating an extra amount of heat which again reduces the performance of the PV system. However, study thermal points, starting from the front-side going through the solar cells to the back-end, must be previously specified in the PV module where the temperature and the heat flow must be analyzed and determined.

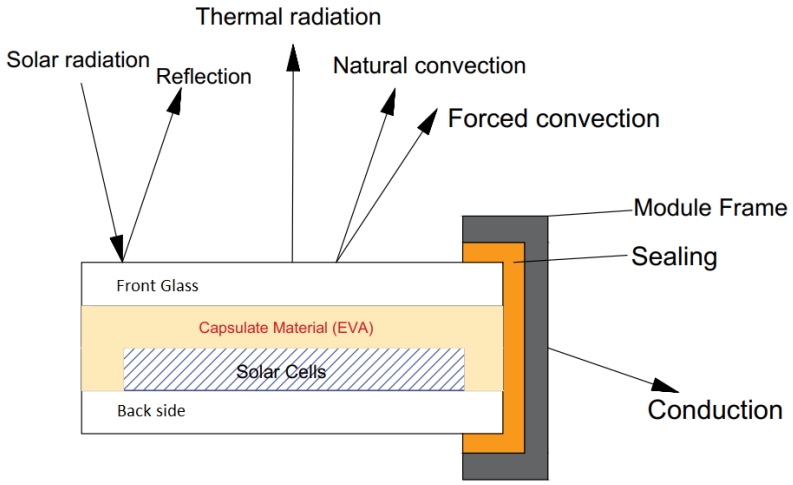

Figure 4.5: Thermal model of the PV module

4.3.1 Conduction

can be defined as the transfer of thermal energy between two objects with different temperatures by means of the direct contact between them. As the heat transfers through the direct collision between molecules. The object with greater area transfers the heat to the one with smaller area. Moreover, as the speed of molecules increases as the faster heat energy transfer. Conduction is the most common type of heat transfer. In particular, when somebody touches a hot metallic surface. However, the conduction process directly depends on the following factors; the instantaneous temperature, the distance, the material properties, and the cross sectional area of each object.

The heat energy transfers directly from the object with higher temperature to the other object that has a lower temperature. The heat transfer will stop once all objects become in equilibrium (No temperature difference). On the other hand, the greater the size and cross-sectional area on an object, the greater the amount of heat energy which is required to heat it. In addition, the smaller the size of an object, the longer the time to lose an object's energy.

In practice, a lot of conduction processes take place within the PV module components resulting different temperature levels among the parts. In particular, there is a conduction

between the front glass and the solar cells matrix. Additionally, there is a conduction between the module itself and its frame but this amount of losses can be neglected, as the contact area between the two layers is very small.

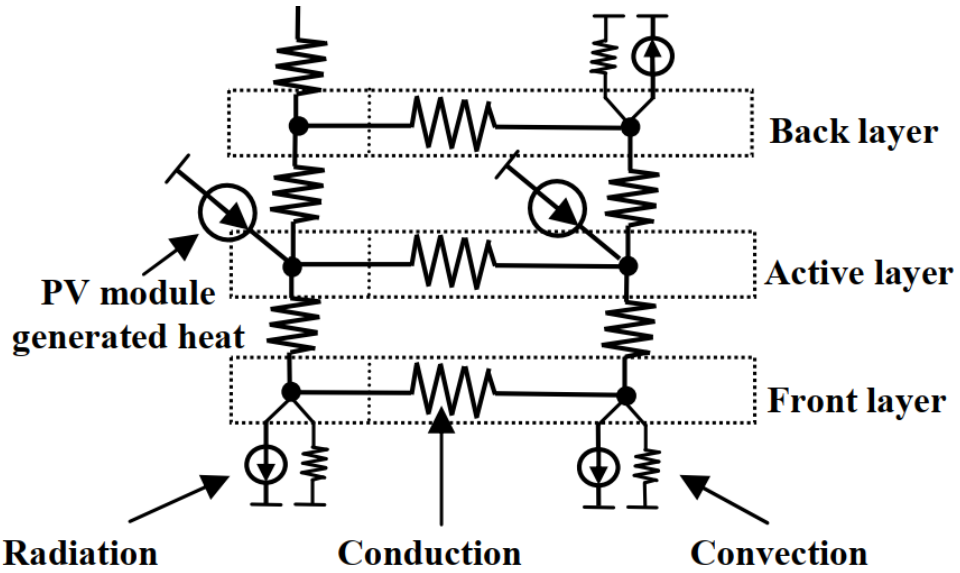

Figure 4.6: Resistor model of the PV module for simulating the heat flow processes; Conduction, Convection and Radiation

The properties of materials are also an important factor of conduction. Namely, a material with a small thickness and a good thermal coefficient transfers heat faster than bigger materials with bad temperature coefficient. The following equation describes the quantity of heat as a function in material properties:

$$Q = [K \cdot A \cdot (T_{hot} - T_{cold})]/d \tag{4.2}$$

Where Q is the transferred heat per unit time, K is the thermal conductivity of the medium, A is the area of medium, T_{hot} is the temperature of the hot object, T_{cold} is the cold object temperature, and d is the gap distance between both objects or the separator thickness.

The conduction heat flow within the PV module can be represented using the resistor capacitor thermal model. Where the resistors represent the losses due to the conduction heat flow (See figure4.6) which also can be expressed using the following equation:

$$R = \frac{1}{K} \cdot \frac{1}{A} \tag{4.3}$$

Where R is the conduction resistance, K is the thermal conductivity of different materials, and A is the cross sectional area of heat pathway.

4.3.2 Convection

is the transfer of heat energy among objects through a fluid or gas. For example, when a hot fluid like a hot oil transfers through a pipe from a point to another it transfer the heat energy to the pipe, this kind of heat transfer is called convection. As the temperature of a

fluid increases the volume also increases with the same factor. The convection process can be formulated by the following equation:

$$Q = h_c \cdot A \cdot (T_s - T_f) \tag{4.4}$$

Where Q is the heat transferred per unit time, h_c is the convection heat transfer coefficient of material, A is the area of heat transfer, T_s is the temperature of surface while T_f is the fluid temperature.

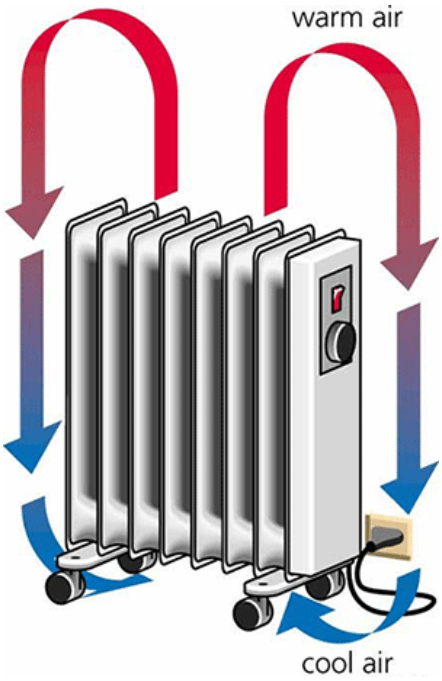

Figure 4.7: Convection heat transfer process

A good example of the convection process is the space heater, which is heating the atmospheric air with in the room. Since the hot surface is the heater and the fluid is air. The heat transfers from the heater to the fluid (Air), and once the air gains the heat, its temperature rises and rise to the top of room while the cold air remains in the bottom until it has been heated.

4.3.3 Radiation

The thermal heat radiation is generated by the electromagnetic waves. These waves can be transmitted through any transparent medium either solid or liquid. The main reason of the solar thermal irradiation is the collision between the atoms and molecules. However, every object radiates thermal energy based on its temperature. The higher the temperature of the object is, the more energy the object will radiate. For instance, the sun is a good examples of the radiation of energy. It radiates thermal energy across the solar system. Every object radiates waves in the room temperature. The frequency and wavelength of these waves are changing continuously based on the object's temperature. For instance, as the temperature increases,

as the wavelengths of the radiation decrease and emitted with higher frequency, which can be calculated using the following equation:

$$Q = e \cdot \sigma \cdot A \cdot (T_r^4 - T_c^4) \tag{4.5}$$

Where Q is the net power of Radiation, e is the emissivity, σ is Stefan's constant, A is the area of radiation, T_r is the radiator temperature, T_c is the receiver of the surrounding temperature.

The maximum and ideal emissivity is 1. And every material has its own value, for example Aluminum has an emissivity of 0.9.

4.4 Calculation of the surface temperature of the Ground/Water

In order to perform a suitable comparison between both the ground-mounted and the floating PV power plants it is necessary to simulate and calculate the surface temperature for the ground (In case of a ground-mounted PV plant) and for the water (In case floating PV plant). A numerical analysis has been performed in order to predict the surface temperature of the ground with the help of the soil/water physical properties i.e. (Conductivity, emissivity, absorptivity, diffusivity and Albedo) which are described for both the ground and the water in table 4.1. The proposed model describes the transient differences of the surface temperature using a set of variables and the climate data such as (Wind speed, solar radiation and ambient temperature).

Table 4.1: The physical properties of the Ground and Water for the aim of performing the numerical analysis

	Ground	Water
Albedo	0.09	0.2
Emissivity	0.85	0.95
Diffusivity (m^3/s)	$1.72 \cdot 10^{-6}$	$0.145 \cdot 10^{-6}$
Absorbtivity	0.91	0.8
Conductivity (W/mK)	1.19	0.6

The model is efficient enough until the stability condition is satisfied. It considers the interaction between the surface of the ground/water and the heat dynamics. The model involves two main different steps: (a) To form the mathematical representation of the heat equation (b) To solve the one dimension heat equation using the proposed numerical model.

The proposed model solves the heat equation using one of the most common methods of solving the differential equations called finite difference method (Also called Bender Schmidt's equation) which is represented by the equation 4.6.

$$T_i^{j+1} = r \cdot T_{i-1}^j + (1 - 2r) \cdot T_i^j + r \cdot T_{i+1}^j \tag{4.6}$$

The model depends on the discretization of the physical domain of the proposed object (Ground or Water). The calculation of any point (using Bender Schmidt's equation) in the next time step $(j+1)$ depends on three points in the previous time step (j) which are at $(i-1$, i and $i+1)$ as shown in figure 4.8

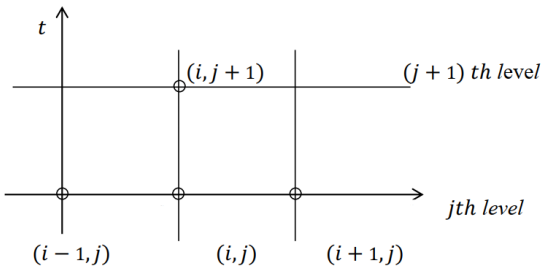

Figure 4.8: Bender Schmidt's representation for the calculation of the next time step $(j+1)$ point

In order to solve the mathematical heat conduction equation 4.7, a forward differencing for the time domain and back differencing for the distance domain were applied to the heat equation 4.7

$$\frac{\partial^2 T(y,t)}{\partial y^2} = \frac{1}{\alpha}\frac{\partial T(y,t)}{\partial t} \tag{4.7}$$

The first boundary condition of the mathematical heat equation is represented by 4.10 which is solved by [41].

$$-k\frac{\partial T}{\partial y}\Big|_{y=0} = h(T_a - T_{y=0}) - \varepsilon\Delta R + \alpha_0 G \tag{4.8}$$

The left hand side of the equation represents the heat conduction through the surface of the Ground/Water depending on the conductivity k of the object. The first term on the right hand side shows the convective heat transfer between the atmosphere $(T_a)$and the surface of the ground $(T_{y=0})$. ΔR is the thermal radiation with the emissivity of the ground/water ε. α_0 is the absorptivity $(1 - Albedo)$ which determines how much solar radiation is absorbed by the object and G is the global radiation on the horizontal plane.

For the simplification the equation 4.10 can be rewritten as

$$-k\frac{\partial T}{\partial y}\Big|_{y=0} = h(T_e - T_{y=0}) \tag{4.9}$$

Where the temperature T_e can be defined as the effective temperature and can be written

$$T_e = T_a - \frac{\varepsilon\Delta R}{h} + \frac{\alpha_0 G}{h} \tag{4.10}$$

Where h represents the radiative h_r and convective h_c heat transfer coefficients.

$$h = h_r + h_c \tag{4.11}$$

The radiative heat transfer coefficient depends on the ambient temperature and can be calculated as the following

$$h_r = 4\varepsilon\sigma T_a^3 \tag{4.12}$$

The convective part h_c can be calculated with respect to the wind speed

$$h_c = 2.8 + 3 \cdot V \tag{4.13}$$

The radiative term ΔR in equation 4.10 can be calculated using the following equation

$$\Delta R = \sigma(T_a^4 - T_{sky}^4) \tag{4.14}$$

4.4.1 Sky temperature

The sky temperature can be calculated quite accurately from the air temperature and and cloudiness of the sky.

$$A(0) = 9.9 \cdot 10^{-}6 \cdot \sigma \cdot T_a^6 \tag{4.15}$$

Where $A(0)$ refers to the thermal atmosphere's radiation at a completely clear sky

$$A(N) = A(0)\Big[1 + a \cdot \frac{N}{8}^2 .5\Big] \tag{4.16}$$

$$a = 2.3 - 7.37 \cdot 10^{-}3 \cdot T_a \tag{4.17}$$

Where N is the degree of the cloudiness of the sky which ranges from 0 (Clear sky) to 8 (Overcast sky)

Figure 4.9 shows a comparison between both the calculated and the measured sky temperatures only during the hottest and coldest days. For the validation of the sky temperature calculation, figure 4.10 illustrates how the calculated sky temperature differs from the actual measure one as the calculated sky temperature in the proposed model was determined at a cloudiness value of 5.

The first boundary condition of the equation 4.6 describes the surface temperature T_0^j

$$T_0^j = \frac{T_1^j + (\frac{h\Delta y}{k})}{1 + \frac{h\Delta y}{k}} \tag{4.18}$$

Where T_e is the effective temperature which is calculated in each time step over the year by the equation 4.10, Δy is the thickness of the laminar in the space domain, k is the conductivity.

The second boundary condition is at the end point of the space domain T_n which is considered as the average annual temperature $\bar{T_e}$

$$T_n^j = \bar{T_e} \tag{4.19}$$

4.4.2 Results

A numerical solution is achieved using Matlab in order to predict the surface temperature of the Ground/Water based on the physical properties of the proposed object. The time step Δt and the space step Δy were 30 s and 0.01 m respectively to maintain the stability condition of the solution ($r \leqslant 0.5$). The physical properties for the ground were assumed constant as $k = 1.19\ W/mK$, $\alpha_0 = 0.91$, $\alpha = 1.72 \cdot 10^{-6}$, $\varepsilon = 0.85$ and for water $k = 0.6\ W/mK$, $\alpha_0 = 0.8$,

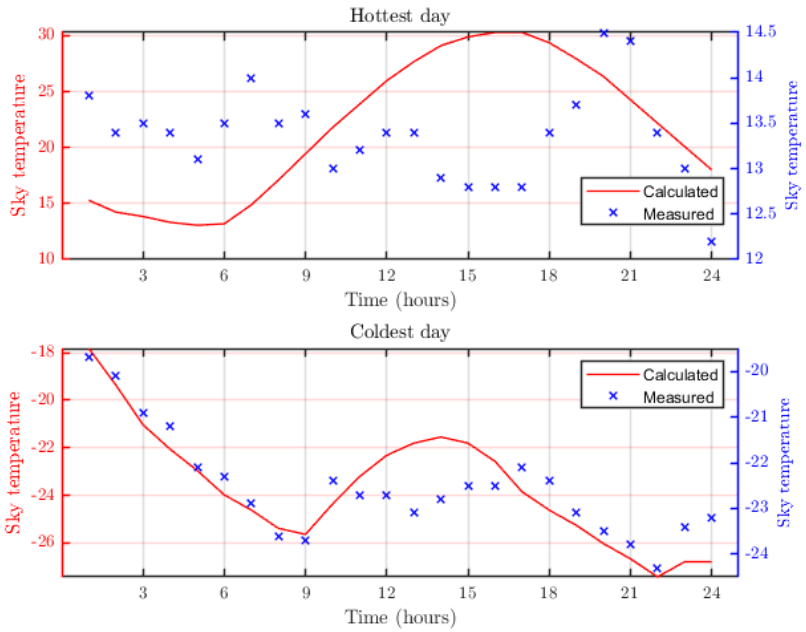

Figure 4.9: The measured and calculated (at N = 5) sky temperature during the hottest and coldest days

$\alpha = 0.145 \cdot 10^{-6}$, $\varepsilon = 0.95$. The simulation model is performed for both the ground and water in order to predict the surface temperature for both of them. Figure 4.15 shows the surface temperature during the hottest and coldest days for the supposed location with the consideration of the above physical properties. Additionally, figure 4.13 illustrates the variation of the surface temperature of both the ground and water over the whole year. The climate data were downloaded for the proposed site in 2015 including the solar radiation, ambient temperature and the wind speed. The hottest and coldest days are 12th of January and the 19th of August respectively. The average annual effective temperature is calculated $\bar{T}_e = 16.89$ °C and $\bar{T}_e = 15.37$ °C for the ground and water respectively.

The variation of the surface temperature of both the ground and water is also studied by the variation of the Albedo values which is illustrated in figure 4.16 and it is shown that, as the Albedo value increases the surface temperature decreases as the absorbtivity of the surface decreases. Furthermore the valued of the thermal conductivity is also varied and surface temperature is studied accordingly, it is found that, as the thermal conductivity increases the surface temperature decreases which is illustrated in figure 4.17. In addition to that, in figure 4.18 it is obvious that the variation of the emissivity value does not affect the variation of the surface temperature as much. The variation of the effective temperature during the hottest and coldest days is illustrated in figure 4.11. In order to validate the behavior of the model another day was chosen to show the surface temperature with respect to the solar radiation for both surfaces Ground and Water as shown in figure 4.19

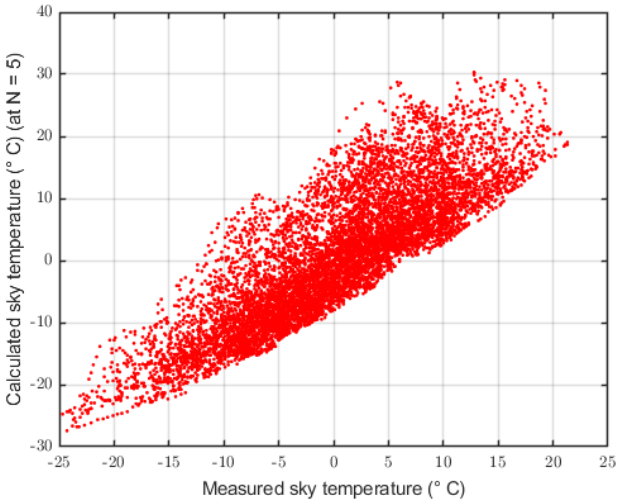

Figure 4.10: A comparison between the calculated at (N=5) and the measured sky temperature over the year

4.5 Instant efficiency of GPV and FPV Modules

As described in section 4.1, that the efficiency is influenced by the deviation in the temperature as well as the global irradiation. Consequently, a simulation model on the PV module is performed in order to predict the instantaneous efficiency, since the module efficiency is all the time changing based on the current irradiation and the ambient temperature. However, the module efficiency calculation is performed during the whole year 2005 for the specified location (Renchen, Germany) for both the ground-mounted PV module as well as the floating type PV module in order to make a comparison between both modules and to realize to what extent the efficiency of the floating PV power plants can sharpen and increase the annual harvested energy.

Generally, the module instantaneous efficiency can be calculated using equation 4.20, T_a and T_{ref} are the ambient and reference temperatures respectively and the temperature coefficient (β)

$$\eta_c = \eta_{Tref} \cdot \Big[1 - \beta_{ref}(T_m - T_{ref})\Big] \tag{4.20}$$

Where η_c is the instantaneous efficiency of the PV module, η_{Tref} is the reference efficiency at the reference temperature T_{ref} at STC.

However, there are a lot of equations which are taken into account to determine the average efficiency as well as the average output power of the PV module over some period shown in table 4.5.

By predicting the efficiency of both the ground-mounted and the floating PV modules, it has been found that the efficiency of the FPV module is considerably higher than efficiency of the ground-mounted PV module as it is shown in figures 4.12a and 4.12b.

Table 4.5 shows some models found in the literature and used to calculate the PV module efficiency based on the available parameters.

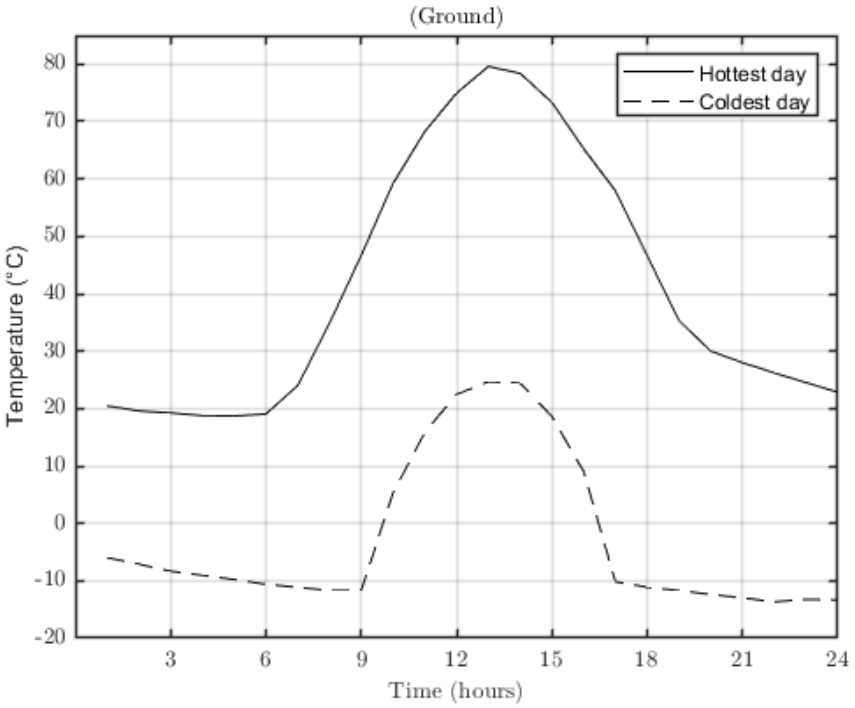

(a)

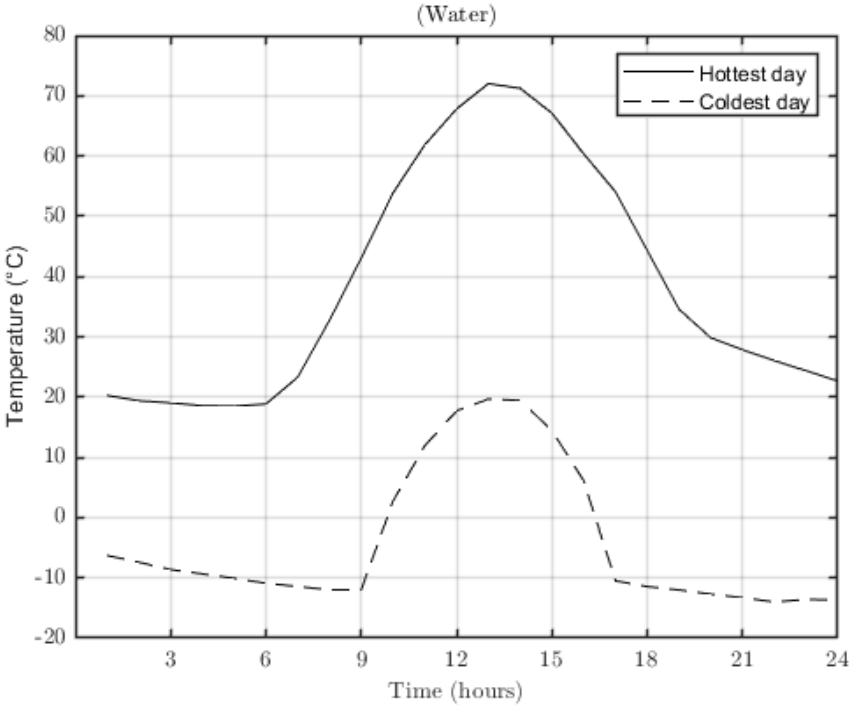

(b)

Figure 4.11: The variation of the effective temperature T_e during the hottest and coldest day for the (a) ground and (b) water surfaces

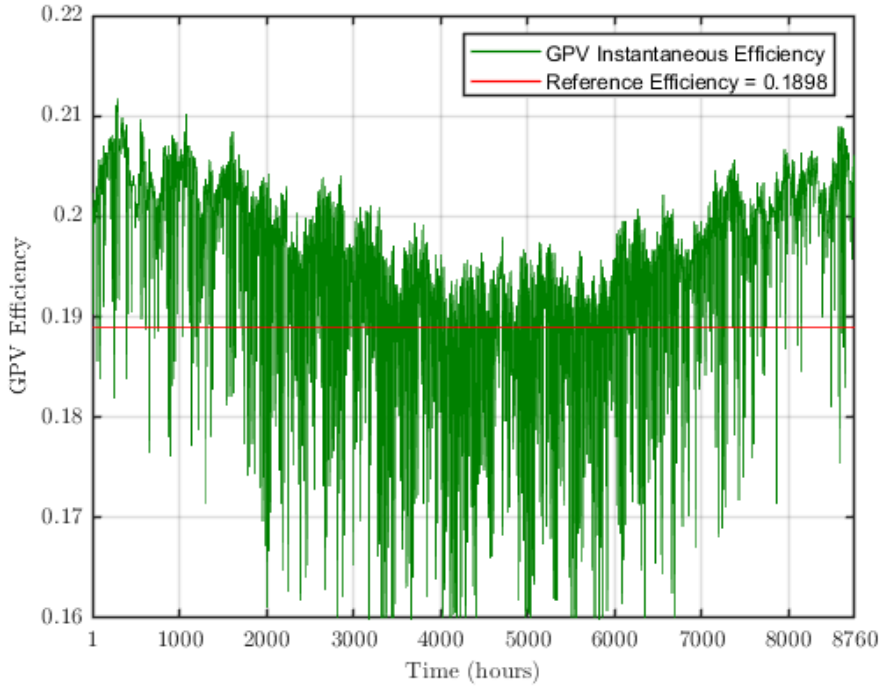

(a)

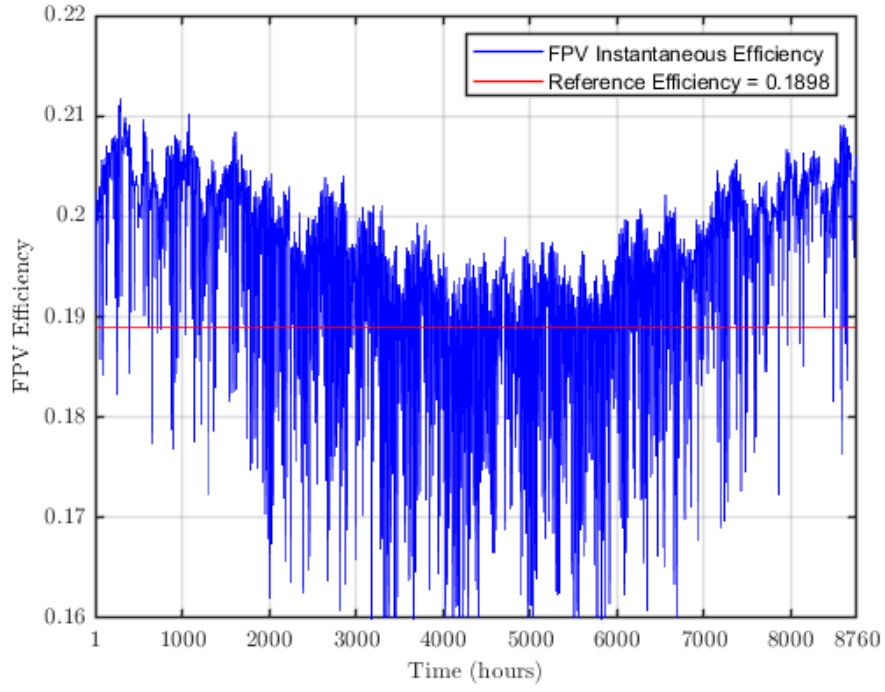

(b)

Figure 4.12: (a) The instantaneous efficiency of the ground-mounted PV module (b) The instantaneous efficiency of the floating PV module

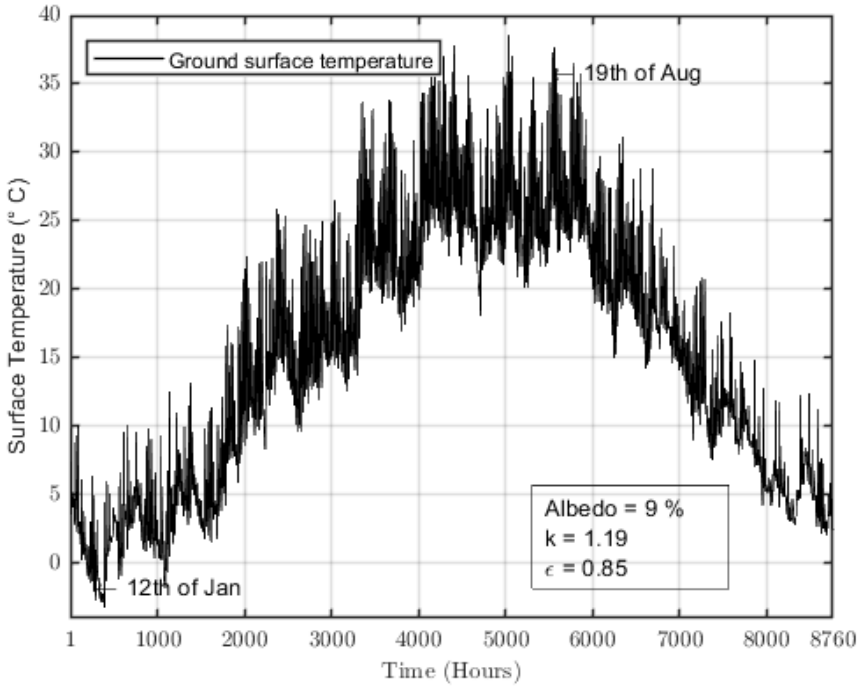

(a) Ground surface temperature

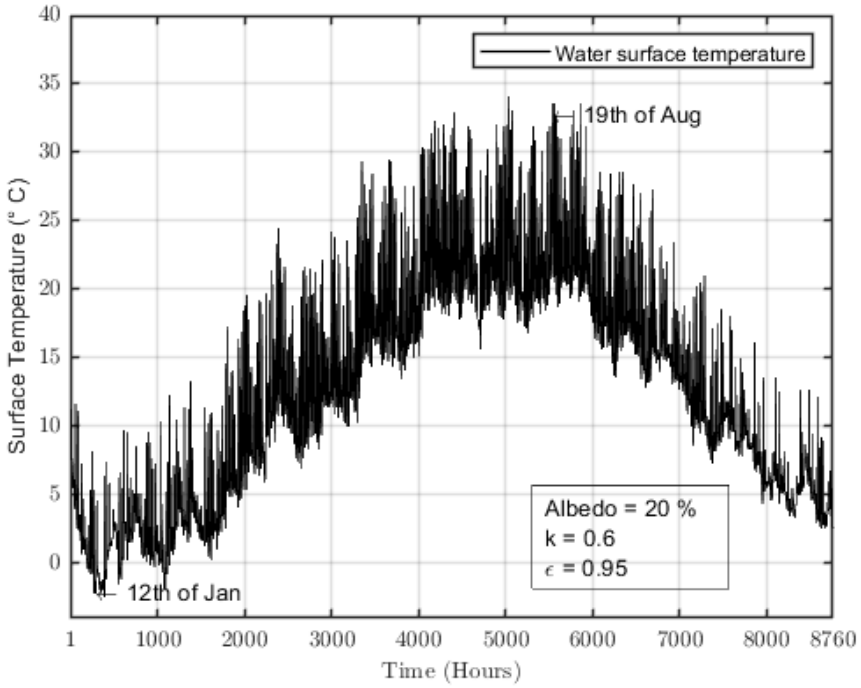

(b) Water surface temperature

Figure 4.13: The variation of the ground surface temperature over the whole year for both the ground and the water surfaces

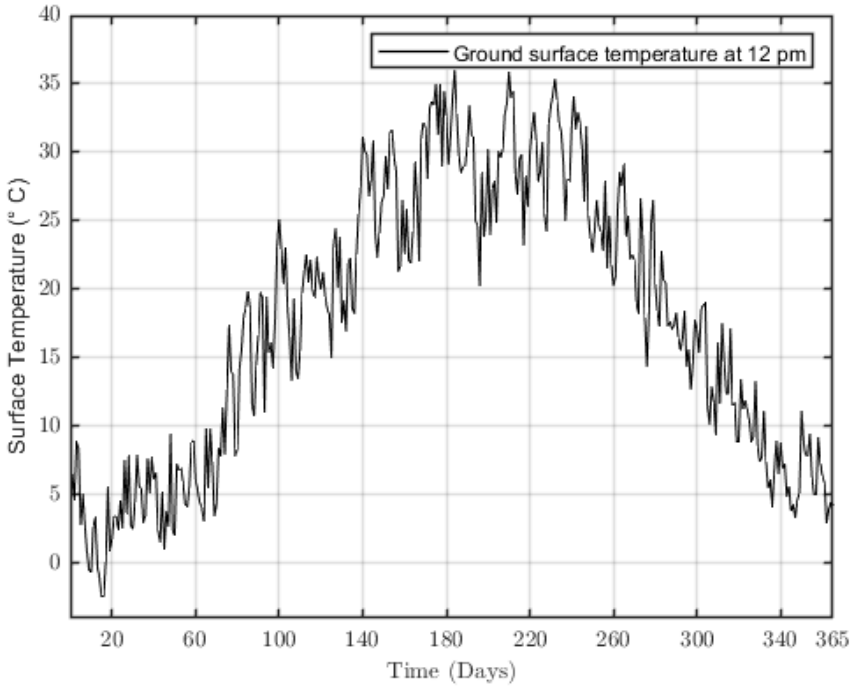

(a) Ground surface temperature

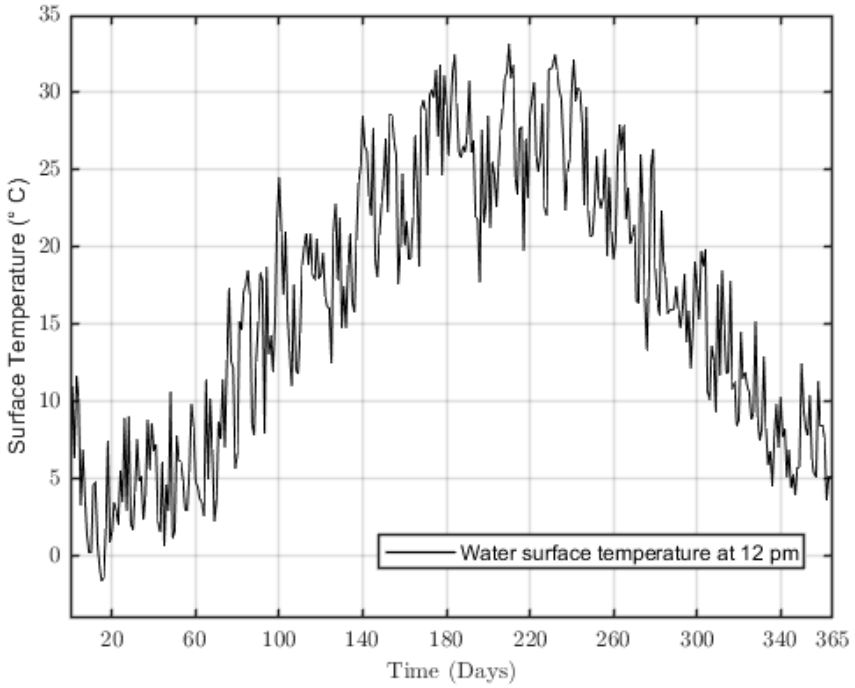

(b) Water surface temperature

Figure 4.14: The variation of the ground surface temperature over the whole year per day at 12 pm for each day for both the ground and the water surfaces

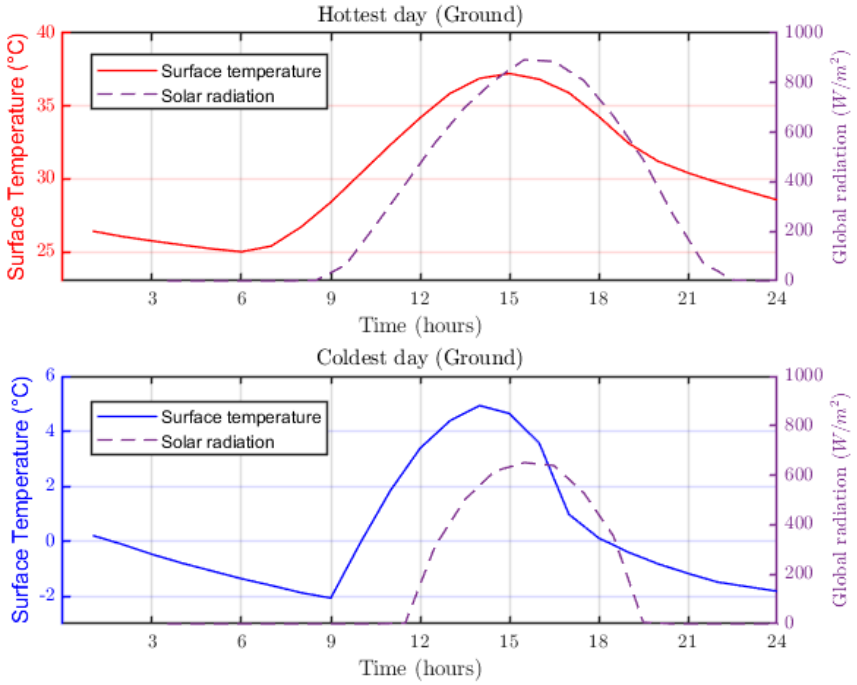

(a) Ground surface temperature

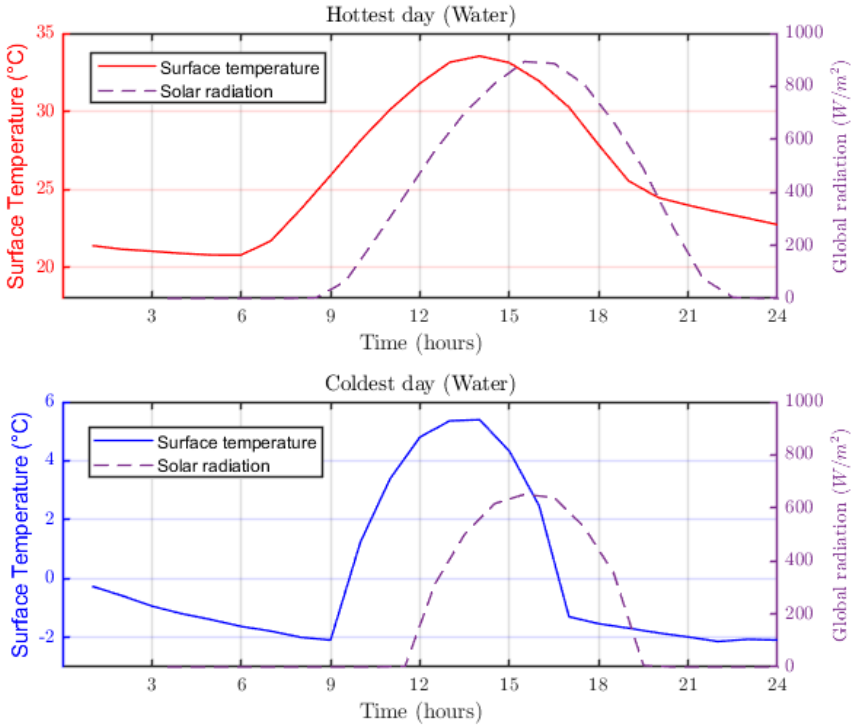

(b) Water surface temperature

Figure 4.15: The surface temperature during the hottest and coldest day for both the ground and water

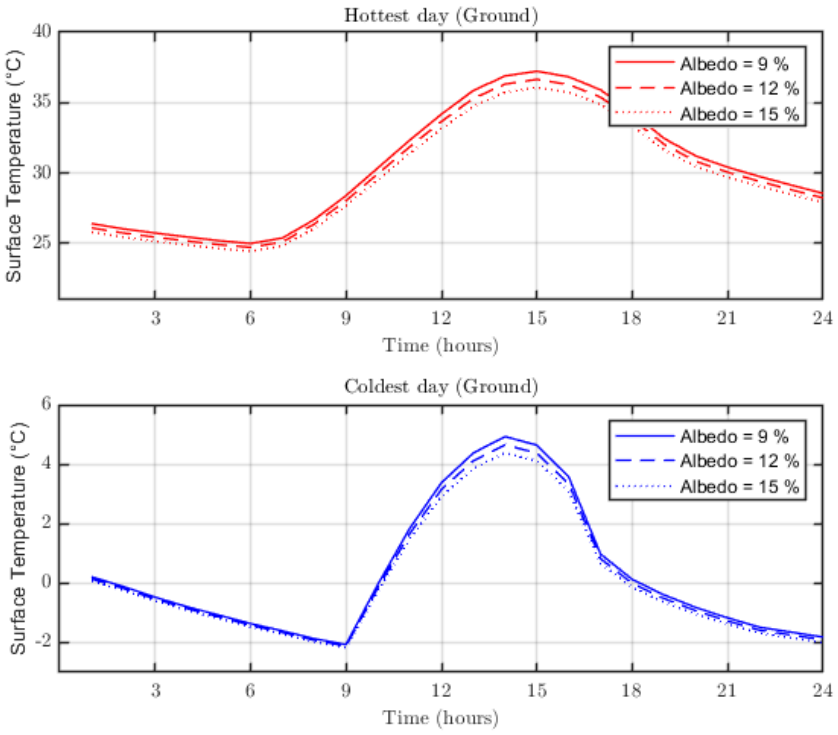

(a) Ground surface temperature

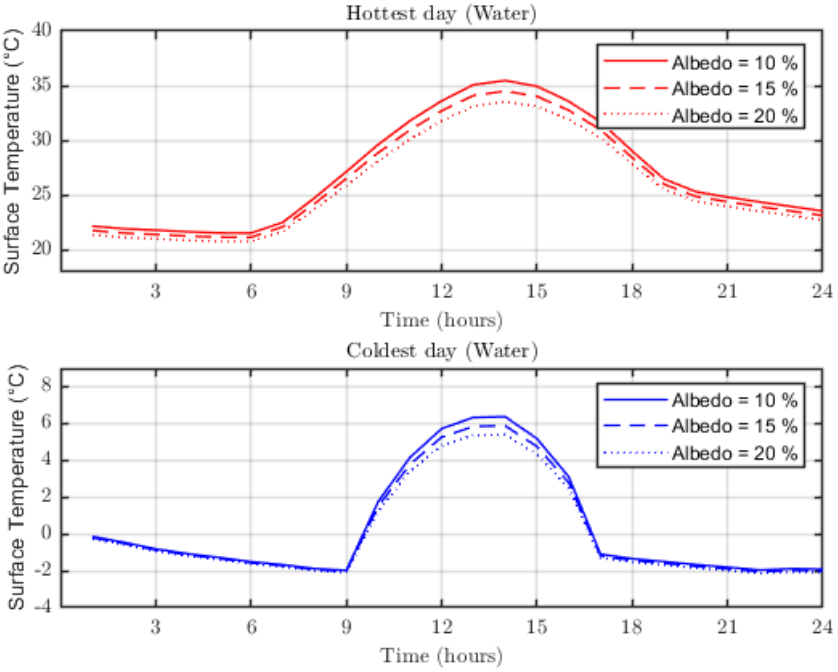

(b) Water surface temperature

Figure 4.16: The surface temperature during the hottest and coldest day for both the ground and water with varied values of Albedo

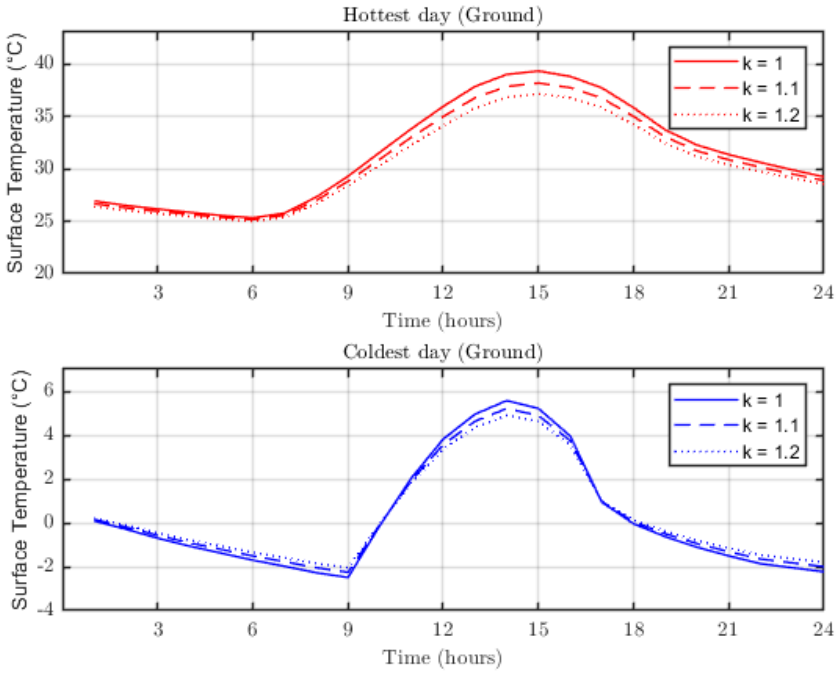

(a) Ground surface temperature

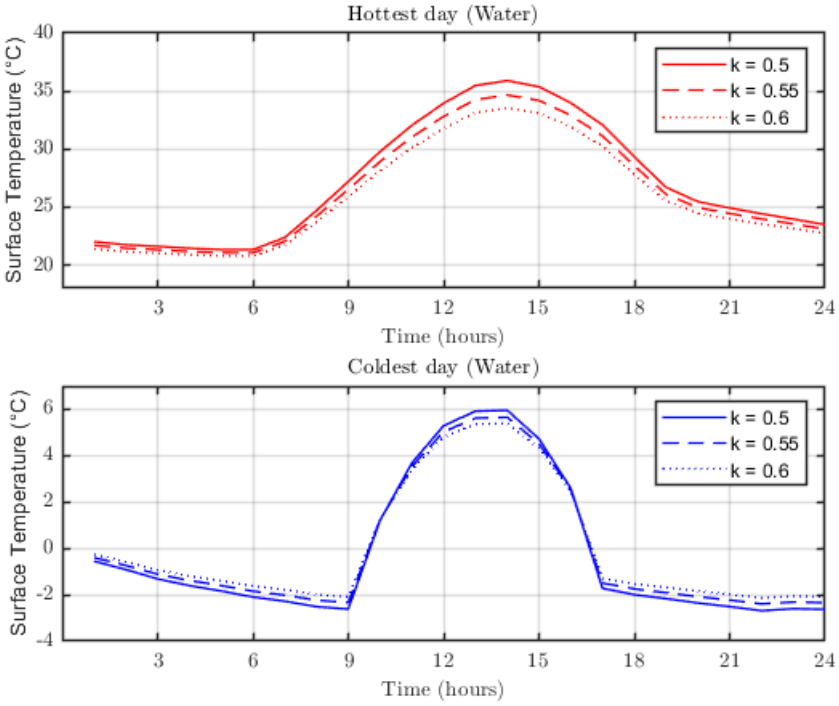

(b) Water surface temperature

Figure 4.17: The surface temperature during the hottest and coldest day for both the ground and water with varied values of thermal conductivity (W/mK)

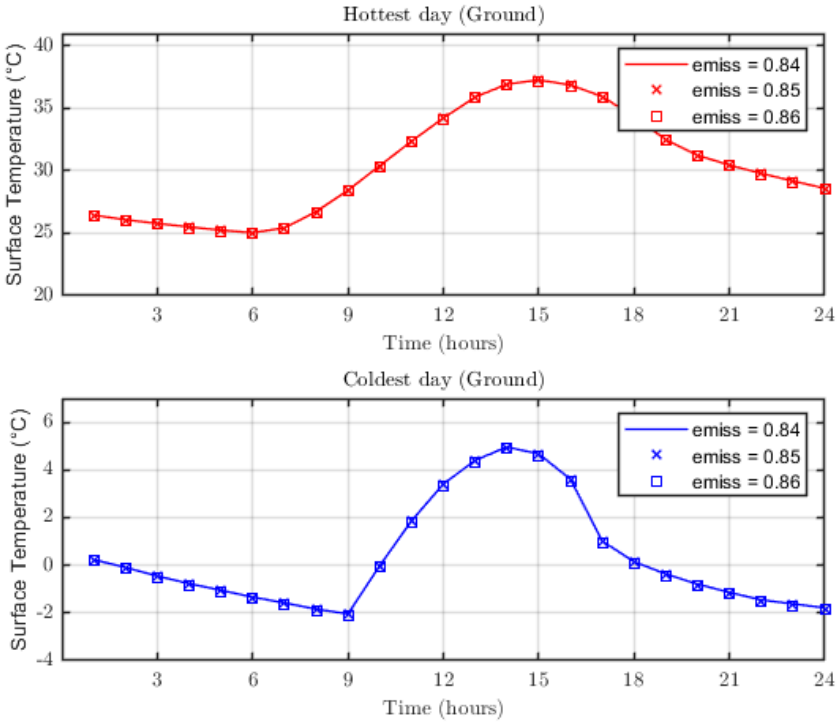

(a) Ground surface temperature

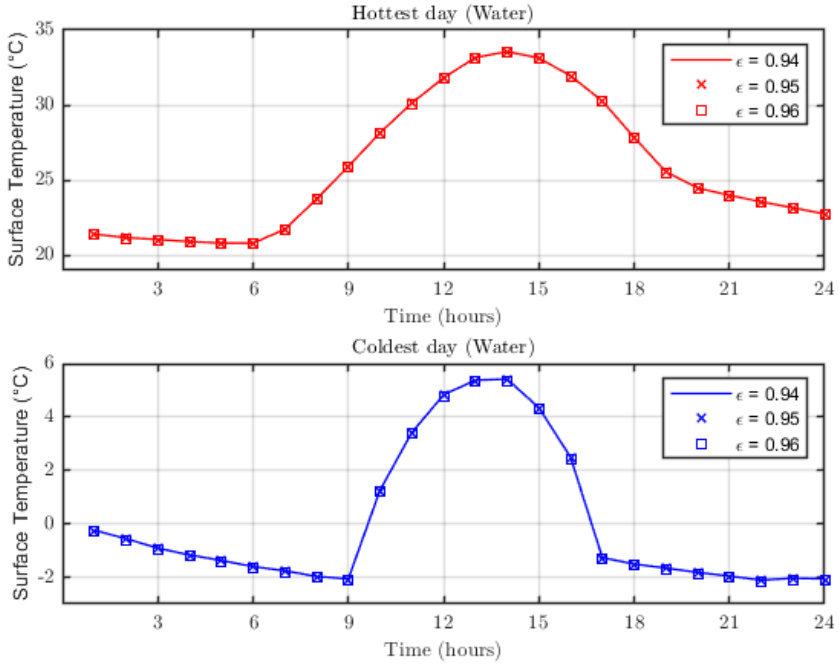

(b) Water surface temperature

Figure 4.18: The surface temperature during the hottest and coldest day for both the ground and water with varied values of the emissivity

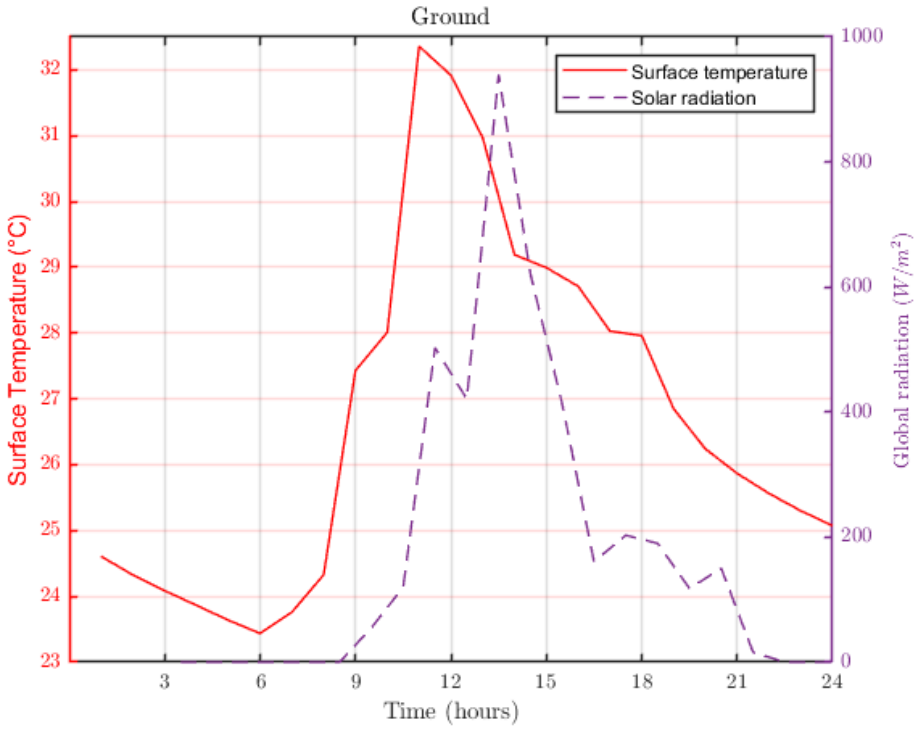

(a) Ground surface temperature

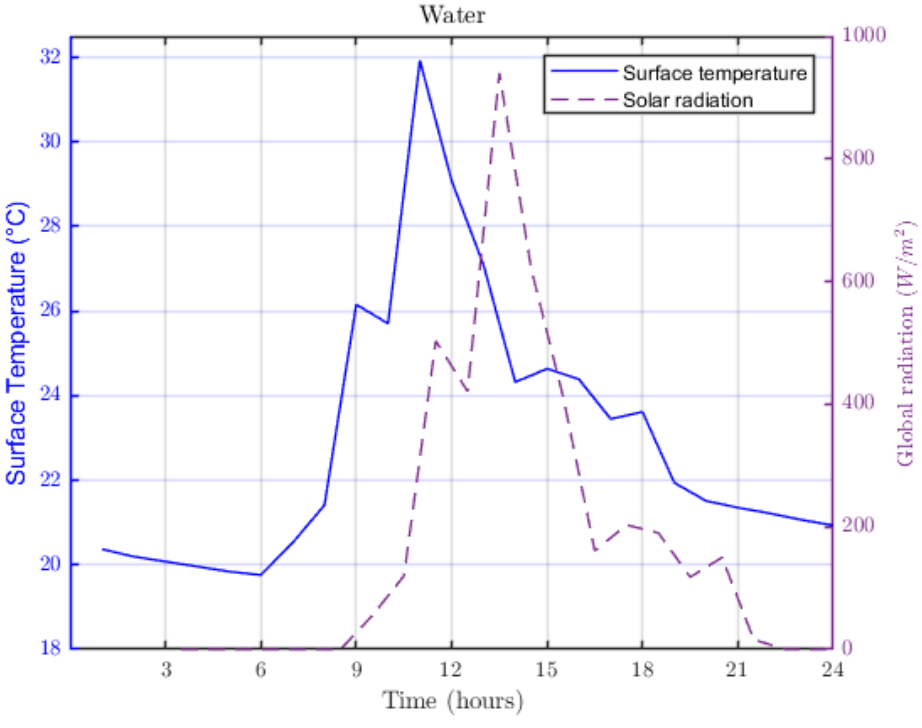

(b) Water surface temperature

Figure 4.19: An illustration of the surface temperature during the a random day for both the ground versus the solar radiations

Table 4.2: Various forms of equations used for calculating the instantaneous efficiency of PV module as a function in radiation and ambient temperature.

Equation	Comments	Reference
$\eta(I(t),T_c) = \eta(I(t),25\check{r}c)[1 + c_3(T_c - 25)]$	$c_3 = -0.5$ (% loss per c) for c-Si -0.41 for thin film cell	[42]
$\eta_T = \eta_0 - k(T^{1/4} - T_0^{1/4})$	$T_0 = 273K$, $k = 22.4$	[43]
$\eta_a = \eta_n \cdot k_\eta \cdot k_\theta \cdot k_\alpha \cdot k_\lambda$ with $k_\eta = 1 - \alpha(T_c - 25)/100$	k_α=Temperature coefficient, k_j,$j = \alpha,\theta,\lambda$ optical, absorption, spectrum correction factors	[44]
$\eta = \eta_{Tref}[1 - \beta_{ref}(T_a - T_{ref}) - \frac{\beta_{ref}\tau\alpha I(t)}{U_L}]$	5% low prediction, $\beta_{ref} \sim 0.004\check{r}c^{-1}$,$\eta_{Tref} = 0.15$ T_{ref} =0°c	[45]
$\overline{\eta} = \eta_{Tref}[1 - \beta_{ref}(\overline{T_a} - T_{ref}) - \frac{\beta_{ref}(\overline{\tau\alpha})\overline{VH_T}}{nU_L}]$	$\overline{\eta}$=Monthly average efficiency, V=dimensionless, $\beta_{ref} \sim 0.004°c^{-1}$	[45]
$\eta_i = \eta_{Tref}[1 - \beta_{ref}(T_{c,i} - T_{ref}) + \alpha \log I_i]$	η_i=hourly efficiency,I_i=incident hourly insol, $\beta_{ref} \sim 0.0045°c^{-1}$,$\alpha \sim 0.12$	[46]
$\eta = \eta_{Tref}[1 - \beta_{ref}(T_c - T_{ref}) + \alpha \log I_{(t)}]$	η=Instant efficiency,$\beta_{ref} \sim 0.0044°c^{-1}$, $\eta_{ref} = 0.125$,$T_{ref} = 25$°c	[47]
$\overline{\eta} = \eta_{Tref}[1 - \beta_{ref}(T_c - T_a) - (T_a - \overline{T_a})$ $-(\overline{T_a} - T_a)]\alpha \log I]$	$\overline{\eta}$ =Monthly average efficiency,$\beta_{ref} \sim 0.0045°c^{-1}$, $\alpha \sim 0.12$	[46]
$\eta = \eta_{ref}[1 - a_1(T_c - T_{ref}) + a_2(\frac{\ln I(t)}{1000})]$	For c-Si $a_1 = 0.005$, $a_2 = 0.052$	[48]
$\eta = a + b\frac{T_{in} - T_a}{I(t)}$	PVT collector, PV cover: $100\% \rightarrow a = 0.123$, $b = -0.464$ $50\% \rightarrow a = 0.121$, $b = -0.450$	[49]

4.6 FPV and GPV Module temperature

The cell temperature is considered a very important factor because it determines all parameters of the PV modules. Since it influences both the output voltage and current as well as the power. Furthermore, as the output power of PV module changes as the maximum power point aslo accordingly changes. Not only that, but also the temperature influences the electrical efficiency of the module as described in section 4.5. The solar cell temperature could be determined by the energy balance. As the solar radiation is partially converted into electricity and partly into heat energy. The heat energy is dissipated by the PV module as thermal losses and the electrical energy is harvested to be either injected directly to the grid or to be consumed by the load.

$$G - G_r - \dot{q} - P_{elec} = 0 \tag{4.21}$$

An energy balance model was built for the PV module in order to predict the module temperature as shown in equation 4.21. Where G is the solar radiation, G_r is the reflected solar radiation away from the solar module which is assumed to be 10 % of the solar radiation, $\dot{q}$ is the net heat transfer which consists of two main components as shown in equation 4.22; the radiative and convective heat transfer components which are calculated by the equations 4.23 and 4.24.

$$\dot{q} = q_c + q_r \tag{4.22}$$

$$q_c = h(T_m - T_a) \tag{4.23}$$

$$q_r = \varepsilon\sigma(T_m^4 - T_g^4) \tag{4.24}$$

Where σ is Stefan's constant, T_m is the PV module temperature, T_g is the ground temperature and h is the heat transfer coefficient.

Then the equation 4.21 can be written as the follwing:

$$G - G_r - h(T_m - T_a) - \varepsilon\sigma(T_m^4 - T_g^4) - P_{elec} = 0 \tag{4.25}$$

Accordingly an iterative solution was performed using Matlab to predict the value of the module temperature whether for the ground-mounted or the floating PV modules.

Figure 4.21 shows the variation of the cell temperature for both the floating and the ground-mounted PV modules over the year 2005. It is clear that, the cell temperature of the FPV module is lower than the GPV cell temperature which higher the module efficiency. As a result, the output power out of the FPV module will be also higher (Will be calculated in section 4.7) and annual harvested energy will increase.

4.7 PV output power as a function of the temperature and the solar irradiation

In order to predict the instant power of the PV module the module temperature must be calculated in advance using the thermal model which is calculated in the previous section and

used in the equation 4.25. Then the equation 4.26 is used to determine the module power [50].

$$P_{Instant} = P_{Tref} \cdot \frac{G}{G_{ref}} \Big[1 + \beta(T_c - T_{ref})\Big] \tag{4.26}$$

Where the $P_{Instant}$ is the instantaneous PV power at a specific cell temperature which were calculated in chapter 4.6, P_{Tref} is the STC power value which stated before by the manufacturer,G is the instantaneous radiation on the solar module surface, G_{ref} is the reference irradiation value which is equal to 1000 W/m^2 (G_{STC} = 1000 W/m^2), β is the temperature coefficient (In this case $\beta = -0.0036$), T_c and T_{ref} are the cell and the reference temperatures respectively [50].

Although there are a lot of formulas used for predicting the output power of PV module, but they must be treated with care, as each of them has its own special conditions. For example, special mounting, tilt angle, height level of the building of integration. Consequently, the simulator should consider all conditions in advance before applying some formula from them. In general, the first priority for the PV designer is to reach the maximum yield from the PV modules, therefore, a proper choice of the PV module as well as the suitable prediction of the PV output power should be done.

Figure 4.22 shows how the PV module power is changing based on the variation of the ambient temperature as well as the cell temperature. It was realized that, because of the reduction of the cell temperature below the STC temperature, the instantaneous values of PV power were more than the reference power stated by the manufacturer.

4.8 Summary and Conclusion

The main purpose of this work is to examine the cell temperature of both the ground mounted and the floating PV modules. As a summary of this work is as follows:

- Simulate the cell temperature of the ground-mounted PV modules.
- Calculate the instantaneous efficiency and power of the ground-mounted PV modules.
- Determine the corresponding instantaneous water temperature.
- Determine the FPV cell temperature.
- Predict the instantaneous efficiency and power of the FPV modules.
- Perform a comparison between both systems (FPV and GPV) with respect to the output power, the instantaneous efficiency and the cell temperature.

Table 4.3 shows the random determined values from the ones which were calculated over the whole year 2005. Based on equation 4.26, the output power of the PV module is highly affected by the change of the irradiation and the module temperature. In particular, for the first day of the year at 12:00 pm, the global irradiation was about 972 W/m^2 and the FPV output power was 304 W_p, although the nominal power stated in advance by the manufacturer is 350 W_p while the GPV module shows a lower output power of 302 W_p. Moreover, in the fourth month both the GPV and FPV modules showed the highest value of the output power of about 336 W_p at a solar radiation of 1036 W/m^2.

Table 4.3: Calculation of the relative power, efficiency and cell temperature of FPV module with a nominal power of 350 W_p that is installed in Renchen, Germany over the whole year 2005 with different values of ambient temperature and global irradiation.

Month	G	T_a	η_{GPV}	η_{FPV}	T_{FPV}	T_{GPV}	P_{GPV}	P_{FPV}
m	W/m^2	$°C$	%	%	$°C$	$°C$	W_p	W_p
3	972	13.1	0.168	0.169	55	56	302	304
4	1036	18.7	0.175	0.175	45	45	336	336
4	1093	22.3	0.162	0.163	64	65	328	329
5	992	18.5	0.178	0.179	40	41	328	328
5	1053	18.4	0.170	0.171	52	53	332	333
5	956	21.3	0.159	0.160	67	69	282	283
5	1064	27.3	0.154	0.155	74	76	304	306
5	971	23.1	0.159	0.159	68	70	285	287
6	1018	21.9	0.153	0.154	77	78	288	290
6	1018	22.3	0.164	0.165	61	62	309	311
6	1034	18	0.172	0.172	50	50	329	330
6	1018	24.4	0.158	0.158	70	71	297	299
6	973	24.9	0.154	0.155	75	76	278	280
6	962	23.2	0.153	0.154	76	77	273	275
7	972	18.2	0.168	0.168	55	56	302	303
7	967	23.4	0.158	0.159	70	71	282	284
8	969	23.5	0.162	0.163	63	64	291	292
8	1011	27.4	0.164	0.165	61	62	307	308
9	1015	18.1	0.165	0.165	60	61	310	311

For a better illustration of the difference between the the GPV and FPV module with respect to the output power and namely the technical potential gained by the floating PV modules the figure 4.20 shows a comparison between both the ground-mounted and the floating PV systems. The curves shown in figure 4.20a represents the whole different values of power of both systems (FPV in red and GPV in blue) sorted from the high to low for the reason of showing how much power can be gained by the floating PV system. On the other hand, figure 4.20b demonstrates the difference between the ground-mounted PV and the floating PV systems (The green shaded area between the two curves). Furthermore, the energy yield for both GPV and FPV plants with 750 kW_p using the same module with 350 kW_p was calculated using the software PVsol, and as shown 4.4 the FPV energy yield with $1,468.86$ is obviously more than that for the GPV with $1,139.60$, additionally, the FPV avoids more CO_2 emission with $404,296$ $kg/year$.

Table 4.4: The technical potential for both GPV and FPV plants [PV*Sol]

Cell technology	GPV	FPV	Gain/Loss (+/-)
Specific Annual Yield (kWh/kW_p)	$1,139.60$	$1,468.86$	$+329.26$
PV Generator Energy ($kWh/year$)	$854,910$	$860,36$	$+5,450$
CO_2 emission avoided($kg/year$)	$401,735$	$404,296$	$+2,561$

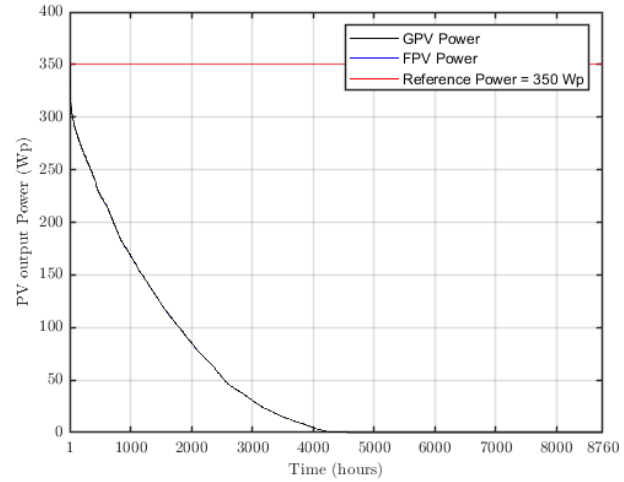

(a)

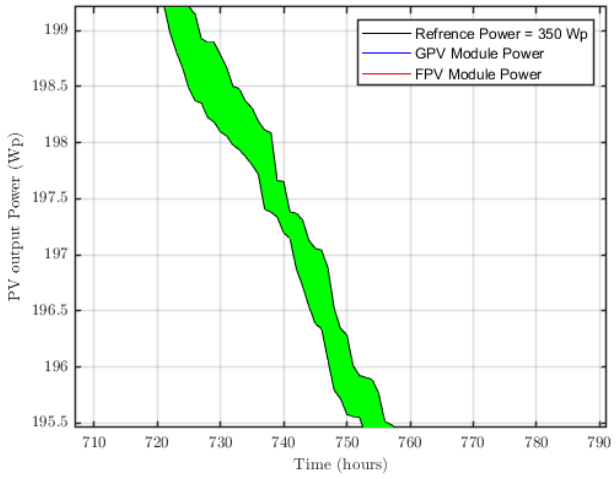

(b)

Figure 4.20: Comparison between the output power values of both FPV and GPV modules sorted from the highest to the lowest (a) The whole values (b) Random selected values.

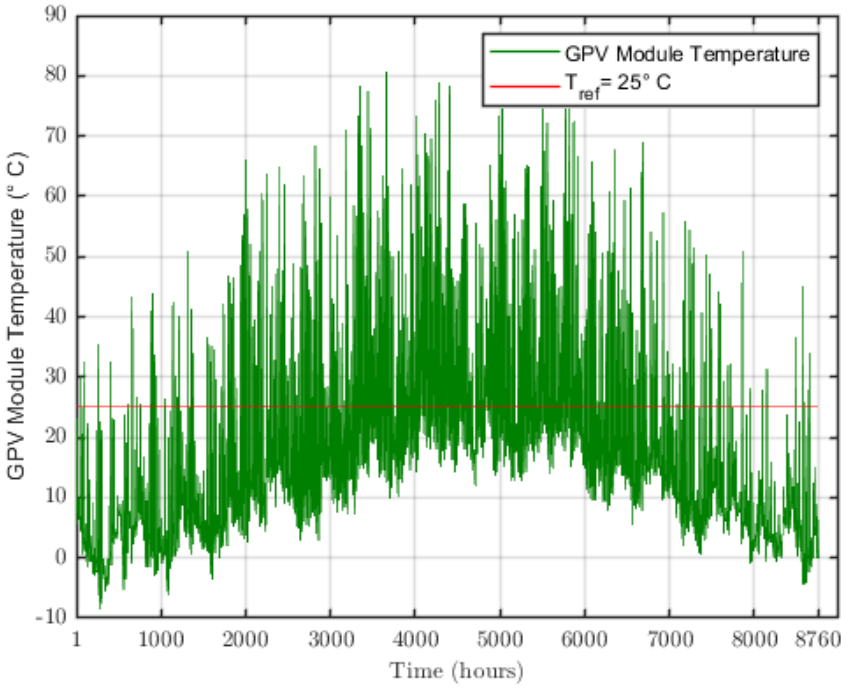

(a)

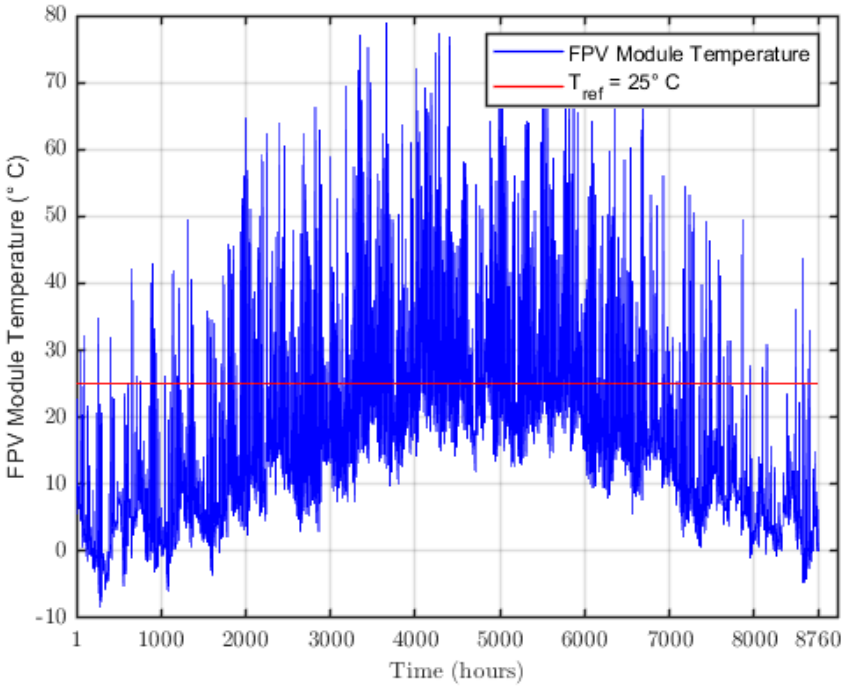

(b)

Figure 4.21: (a) The instantaneous temperature of the ground-mounted PV module (b) The instantaneous temperature of the floating PV module

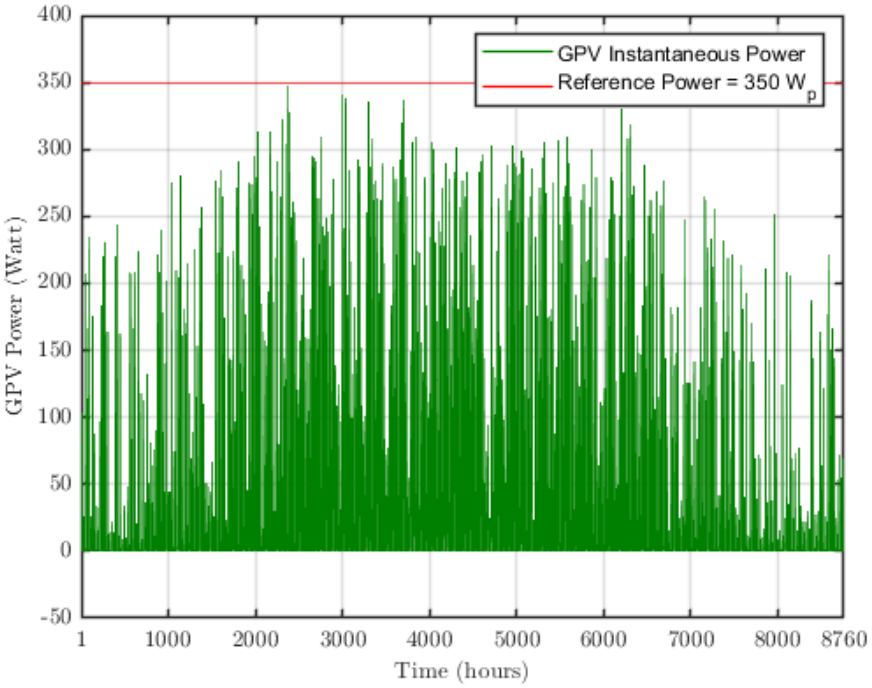

(a)

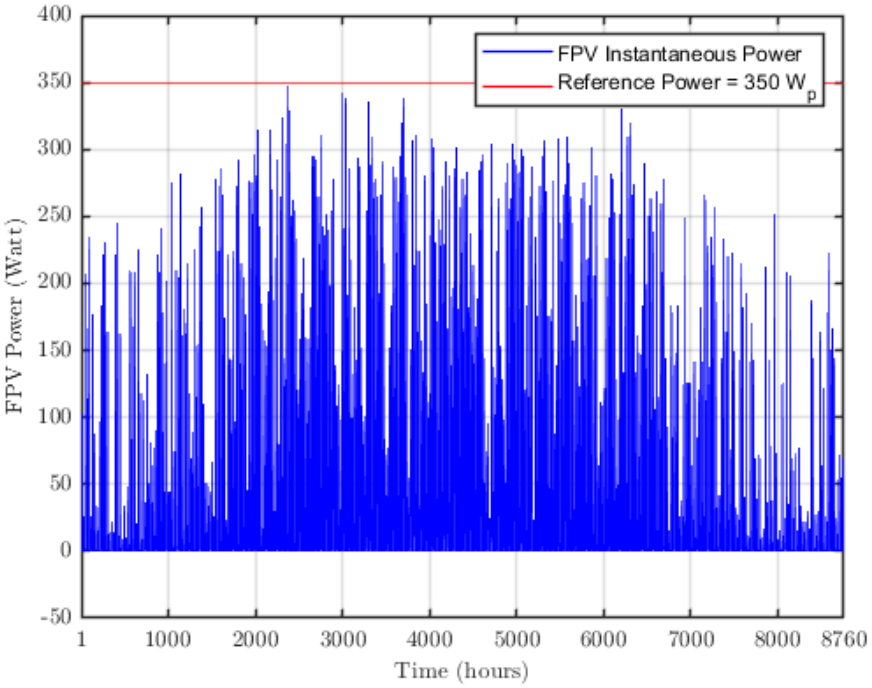

(b)

Figure 4.22: (a) The instantaneous power of the ground-mounted PV module (b) The instantaneous power of the floating PV module

References

[1] Ciel and terre, www.ciel-et-terre.net.

[2] M. E. Taboada, L. Cáceres, T. A. Graber, H. R. Galleguillos, L. F. Cabeza, R. Rojas, Solar water heating system and photovoltaic floating cover to reduce evaporation: Experimental results and modeling, Renewable energy 105 (2017) 601–615.

[3] W. Charles Lawrence Kamuyu, J. R. Lim, C. S. Won, H. K. Ahn, Prediction model of photovoltaic module temperature for power performance of floating PVs, Energies 11 (2) (2018) 447.

[4] Floating solar, www.floating-solar.com/technologies.html.

[5] M. Rosa-Clot, G. M. Tina, Submerged and Floating Photovoltaic Systems: Modelling, Design and Case Studies, Academic Press, 2017.

[6] Y. Choi, A case study on suitable area and resource for development of floating photovoltaic system, International Journal of Electrical, Computer, Energetic, Electronic and Communication Engineering 8 (5) (2014) 828–832.

[7] R. Cazzaniga, M. Rosa-Clot, P. Rosa-Clot, G. M. Tina, Floating tracking cooling concentrating (FTCC) systems, in: 2012 38th IEEE Photovoltaic Specialists Conference, IEEE, 2012, pp. 000514–000519.

[8] I. E. Commission, et al., IEC 60529: degrees of protection provided by enclosures (IP code), See Appendix (1989).

[9] M. D. Kempe, Modeling of rates of moisture ingress into photovoltaic modules, Solar Energy Materials and Solar Cells 90 (16) (2006) 2720–2738.

[10] R. W. Andrews, J. M. Pearce, The effect of spectral albedo on amorphous silicon and crystalline silicon solar photovoltaic device performance, Solar Energy 91 (2013) 233–241.

[11] k2-systems.commounting systems for solar technology, www.k2-systems.com/de/start.

[12] Solarmarkt, www.solarmarkt.ch/de.

[13] A. F. Castanheira, J. F. Fernandes, P. C. Branco, Demonstration project of a cooling system for existing pv power plants in portugal, Applied energy 211 (2018) 1297–1307.

[14] T. Huld, A. M. G. Amillo, Estimating pv module performance over large geographical regions: The role of irradiance, air temperature, wind speed and solar spectrum, Energies 8 (6) (2015) 5159–5181.

[15] V. Durković, Ž. Đurišić, Analysis of the potential for use of floating PV power plant on the Skadar Lake for electricity supply of aluminium plant in Montenegro, Energies 10 (10) (2017) 1505.

[16] F. Möller, Einführung in die meteorologie, Tech. rep., Bibliographisches Institut (1973).

[17] E. Dobos, 'w11 45 46 47 4s (2003).

[18] M. S. M. Azmi, M. Y. H. Othman, M. H. H. Ruslan, K. Sopian, Z. A. A. Majid, Study on electrical power output of floating photovoltaic and conventional photovoltaic, in: AIP Conference Proceedings, Vol. 1571, American Institute of Physics, 2013, pp. 95–101.

[19] International energy agency (iea 2020), `https://www.iea.org/reports/world-energy-balances-overview`.

[20] Japan asia investment co ltd, `www.jaic-vc.co.jp/eng/index.html`.

[21] E. S. M. A. Program, S. E. R. I. of Singapore, Where sun meets water: Floating solar handbook for practitioners (2019).

[22] Y.-K. Choi, N.-H. Lee, K.-J. Kim, Empirical Research on the efficiency of Floating PV systems compared with Overland PV Systems, in: Proceedings, The 3rd International Conference on Circuits, Control, Communication, Electricity, Electronics, Energy, System, Signal and Simulation, Vol. 25, 2013, pp. 284–289.

[23] K. Trapani, M. Redón Santafé, A review of floating photovoltaic installations: 2007–2013, Progress in Photovoltaics: Research and Applications 23 (4) (2015) 524–532.

[24] R. S. Spencer, J. Macknick, A. Aznar, A. Warren, M. O. Reese, Floating photovoltaic systems: assessing the technical potential of photovoltaic systems on man-made water bodies in the continental United States, Environmental science & technology 53 (3) (2018) 1680–1689.

[25] L. Liu, Q. Wang, H. Lin, H. Li, Q. Sun, et al., Power generation efficiency and prospects of floating photovoltaic systems, Energy Procedia 105 (2017) 1136–1142.

[26] Y.-G. Lee, H.-J. Joo, S.-J. Yoon, Design and installation of floating type photovoltaic energy generation system using FRP members, Solar Energy 108 (2014) 13–27.

[27] N. Yadav, M. Gupta, K. Sudhakar, Energy assessment of floating photovoltaic system, in: 2016 International Conference on Electrical Power and Energy Systems (ICEPES), IEEE, 2016, pp. 264–269.

[28] Z. A. A. Majid, M. H. Ruslan, K. Sopian, M. Y. Othman, M. S. M. Azmi, Study on performance of 80 watt floating photovoltaic panel, Journal of Mechanical Engineering and Sciences 7 (1) (2014) 1150–1156.

[29] S. Odeh, M. Behnia, Improving photovoltaic module efficiency using water cooling, Heat Transfer Engineering 30 (6) (2009) 499–505.

[30] Pv magazine, `www.pv-magazine.de`.

[31] J. A. Kratochvil, W. E. Boyson, D. L. King, Photovoltaic array performance model., Tech. rep., Sandia National Laboratories (2004).

[32] S. Nann, K. Emery, Spectral effects on pv-device rating, Solar Energy Materials and Solar Cells 27 (3) (1992) 189–216.

[33] S. A. Kalogirou, L. Aresti, P. Christodoulides, G. Florides, The effect of air flow on a building integrated pv-panel, Procedia IUTAM 11 (2014) 89–97.

[34] Y. Sheikh, A. Butt, K. Paracha, A. Awan, A. Bhatti, M. Zubair, An improved cooling system design to enhance energy efficiency of floating photovoltaic systems, Journal of Renewable and Sustainable Energy 12 (5) (2020) 053502.

[35] Y. Irwan, W. Leow, M. Irwanto, A. Amelia, N. Gomesh, I. Safwati, et al., Indoor test performance of pv panel through water cooling method, Energy Procedia 79 (2015) 604–611.

[36] K. Sayed, M. Abdel-Salam, M. Ahmed, A. A. Ahmed, Electro-thermal modeling of solar photovoltaic arrays, in: ASME International Mechanical Engineering Congress and Exposition, Vol. 54907, 2011, pp. 1143–1149.

[37] S. Winter, D. Friedrich, A. Sperling, Effects of the new standard iec 60904-3: 2008 on the calibration results of common solar cell types, in: 24th European Photovoltaic Solar Energy Conference, 2009, pp. 21–25.

[38] T. Huld, G. Friesen, A. Skoczek, R. P. Kenny, T. Sample, M. Field, E. D. Dunlop, A power-rating model for crystalline silicon pv modules, Solar Energy Materials and Solar Cells 95 (12) (2011) 3359–3369.

[39] M. Ačanski, J. Popović-Gerber, B. Ferreira, Thermal modeling of the module integrated dc-dc converter for thin-film pv modules, in: Proceedings of 14th International Power Electronics and Motion Control Conference EPE-PEMC 2010, IEEE, 2010, pp. T12–160.

[40] L. Oliverio, G. Timò, A. Minuto, P. Groppelli, Thermal simulations of a cpv point focus module using comsol multiphysics, Solar Energy Technology (2010) 55–64.

[41] S. Bharadwaj, N. Bansal, Temperature distribution inside ground for various surface conditions, Building and Environment 16 (3) (1981) 183–192.

[42] H. Mohring, D. Stellbogen, R. Schäffler, S. Oelting, R. Gegenwart, P. Konttinen, T. Carlsson, M. Cendagorta, W. Herrmann, Outdoor performance of polycrystalline thin film pv modules in different european climates, in: Proceedings of the 19th European Photovoltaic Solar Energy Conference, 2004, pp. 2098–2101.

[43] N. Ravindra, V. Srivastava, Temperature dependence of the maximum theoretical efficiency in solar cells, SoCe 1 (1979) 107–109.

[44] N. Aste, G. Chiesa, F. Verri, Design, development and performance monitoring of a photovoltaic-thermal (pvt) air collector, Renewable energy 33 (5) (2008) 914–927.

[45] M. Siegel, S. Klein, W. Beckman, A simplified method for estimating the monthly-average performance of photovoltaic systems, Solar Energy 26 (5) (1981) 413–418.

[46] D. Evans, Simplified method for predicting photovoltaic array output, Solar energy 27 (6) (1981) 555–560.

[47] G. Notton, C. Cristofari, M. Mattei, P. Poggi, Modelling of a double-glass photovoltaic module using finite differences, Applied thermal engineering 25 (17-18) (2005) 2854–2877.

[48] A. DUMAS, F. Draghetti, Theoretical and experimental analysis of two passive cooling systems for the solar cells without concentration, in: Internattional Solar Energy Society Congress 1981, Vol. 4, Pergamon Press, 1981, pp. 2908–2912.

[49] J. Ji, J. Han, T. Chow, C. Han, J. Lu, W. He, Effect of flow channel dimensions on the performance of a box-frame photovoltaic/thermal collector, Proceedings of the Institution of Mechanical Engineers, Part A: Journal of Power and Energy 220 (7) (2006) 681–688.

[50] G. N. Tiwari, S. Dubey, Fundamentals of photovoltaic modules and their applications, Royal Society of Chemistry, 2009.